Application of Nuclear Magnetic Resonance Spectroscopy to Pharmaceutical and Agricultural Research

Kanaori, Kenji

(Degree)
博士（理学）

(Date of Degree)
1996-09-18

(Date of Publication)
2012-07-06

(Resource Type)
doctoral thesis

(Report Number)
乙2070

(JaLCDOI)
https://doi.org/10.11501/3129833

(URL)
https://hdl.handle.net/20.500.14094/D2002070

神戸大学博士論文

Application of Nuclear Magnetic Resonance Spectroscopy to Pharmaceutical and Agricultural Research

平成　８年　８月

金折　賢二

神戸大学博士論文

Application of Nuclear Magnetic Resonance Spectroscopy
to Pharmaceutical and Agricultural Research

(核磁気共鳴分光法の医農薬研究への応用)

Kenji Kanaori

1996

CONTENTS

General introduction

Nuclear Magnetic Resonance (NMR) spectroscopy has been used for the pharmaceutical and agricultural research and development. In particular, since 1984 when a protein structure determination by NMR spectroscopy in solution was established (Wüthrich et al., 1982), NMR has provided a more reliable platform for rational drug design and the engineering of novel protein functions. In addition to its key role in academic institutions, the structure determination of proteins, nucleic acids and other classes of biomolecules has, therefore, become a discipline that is also actively pursued in profit-oriented organizations, especially in the major pharmaceutical companies. Therefore, in the biotechnical and biomedical fields, NMR is considered to be taken as a tool merely for the structure determination of the biomacromolecules. However, there exist many biological macromolecules whose atomic resolution study of the three-dimensional structure is impossible because of a small amount, high molecular weight (> 30,000), aggregation, etc. This thesis presents other useful applications of NMR to biological systems where the precise tertiary structure cannot be determined.

Peptide aggregation and precipitation are major biomedical problems. These precipitates are the cause of serious diseases, e.g. Down's syndrome and Alzheimer's disease (Glenner et al., 1984; Masters et al., 1985). Protein aggregation is also an important biotechnological problem. During the production of recombinant proteins, precipitates of protein, called inclusion bodies, often build up within the host cell. Protein drugs currently on the market continue to have aggregation problems: implantable and portable delivery systems for insulin are commonly obstructed by insulin precipitates (Lougheed et al., 1980). For another example, it has been known that human calcitonin (hCT), a drug for

osteoporosis, easily associates and precipitates as insoluble fibrils in aqueous solution (Sieber et al., 1970). HCT given by a venous injection, precipitates in a syringe, which is disadvantageous in therapeutic use. In Chapter 1, the fibrillation of hCT was investigated by analyzing time-course of two-dimensional (2D) ^{1}H NMR spectra. The aggregation process under the above medical conditions has been examined by electron microscopy, turbidity, circular dichroism, fluorescence and fourier transform infrared spectroscopy (Arvinte et al., 1994; Ferrone et al., 1980, 1985; Yoshida et al., 1993), but scarcely by NMR spectroscopy, because of signal broadening accompanied by aggregation. In order to develop long time stable derivatives of hCT, it is necessary to obtain the structural aspects so as to residues actually involved in the fibrillation. To our knowledge this is the first attempt to measure the time-course of aggregation process by 2D NMR methods, and to clarify the mechanism of the fibrillation at atomic level.

In Chapter 2, *cabbage* histidinol dehydrogenase (HDH, MW 100,000), which catalyzes two sequential oxidation reactions to yield L-histidine from L-histidinol *via* L-histidinal (Adams, 1955) was studied by ^{113}Cd NMR. It is anticipated that the inhibition of histidine biosynthesis hinders the growth of plant, and that an inhibitor against *cabbage* HDH could become a lead compound of a novel and promising herbicide. Structural information about the catalytic site is important for design of an inhibitor. However, HDH is too large to be examined by multi-dimensional NMR spectroscopy, and its X-ray crystallography study has not been reported yet.

HDH contains 1 mol of Zn(II) per mol of subunit, and removal of this metal abolishes the enzymatic activity (Lee & Grubmeyer, 1987), suggesting that the metal ion of HDH plays a significant role in the reaction. Cd(II) can often be substituted for Zn(II) at the active site of the

metalloenzymes with retention of activity (Chlebowski & Coleman, 1976; Omburo et al., 1993). Hence metal ions in several zinc metalloenzymes have been explored by ^{113}Cd NMR spectroscopy (Summers, 1988). The chemical shift and line width of ^{113}Cd are sensitive to the number, type, geometry, and dissociation constant of its ligands. For proteins whose X-ray structural data are not available, ^{113}Cd NMR has given us a first-approximation of the ligands at the metal binding sites. In many cases, ^{113}Cd NMR spectroscopy can provide new insights into protein-substrate interactions, conformational changes, and metal displacement reactions.

In the case of HDH, on substitution of $^{113}Cd(II)$ with Zn(II), the enzyme ([^{113}Cd]HDH) showed similar catalytic activity, and ^{113}Cd NMR spectra of [^{113}Cd]HDH were measured under various conditions. The role of the metal ion in the catalytic reaction of HDH will be discussed.

References

Adams, E. (1955) *J. Biol. Chem. 217*, 25-344.

Arvinte, T., Cudd, A., & Drake, A. F. (1993) *J. Biol. Chem. 268*, 6415-6422.

Chlebowski, J. F., & Coleman, J. E. (1976) *J. Biol. Chem. 251,* 1202-1206.

Ferrone, F. A., Hofrichter, J., Sunshine, H. R., & Eaton, W. A. (1980) *Biophys. J. 32*, 361-380.

Ferrone, F. A., Hofrichter, J., & Eaton, W. A. (1985) *J. Mol. Biol. 183*, 611-631.

Glenner, G. G., & Wong, C. W. (1984) *Biochem. Biophys. Res. Commun.* 120, 885-890.

Lee, S. Y., & Grubmeyer, C. T. (1987) *J. Bacteriol. 169*, 3938-3944.

Lougheed, W., Woulfe-Flanagan, H., Clement, J., & Albisser, F. (1980) *Diabetologia 19,* 1-9.

Masters, C. L., Simmes, G., Weinman, N. A., Multhaup, G., McDonald, B. L., & Beyreuther, K. (1985) *Proc. Natl. Acad. Sci. U. S. A. 82,* 4254-4249.

Omburo, G. A., Mullins, L. S., & Raushel,. F. M. (1993) *Biochemistry 32,* 9148-9155.

Sieber, P., Riniker, B., Brugger, M., Kamber, B., & Rittel, W. (1970) *Helv. Chim. Acta 53*, 2135-2150.

Summers, M. F. (1988) *Coord. Chem. Rev. 86*, 43-134.

Wüthrich, K., Wider, G., Wagner, G., & Braun, W. (1982) *J. Mol. Biol. 155*, 311-319.

Yoshida, K., Shibata, T., Masai, J., Sato, K., Noguti, T., Go, M., & Yanagawa, H. (1993) *Biochemistry 32*, 2162-2166.

Chapter 1

Study of Human Calcitonin Fibrillation by ^1H NMR Spectroscopy

Abbreviations

CT, calcitonin; hCT, human calcitonin; CD, circular dichroism; FTIR, fourier transform infrared spectroscopy; sCT, salmon calcitonin; TFE, 2,2,2-trifluoroethanol; MeOH, methanol; SDS, sodium dodecyl sulfate; DMSO, dimethylsulfoxide; t_f, fibrillation time; 1D, one-dimensional; 2D, two-dimensional; DQFCOSY, double-quantum filtered correlated spectroscopy; HOHAHA, homonuclear Hartmann-hahn spectroscopy; NOESY, nuclear Overhauser enhancement spectroscopy; TPPI, time-proportional phase incrementation method; ROESY, rotating frame nuclear Overhauser enhancement spectroscopy; NOE, nuclear Overhauser enhancement; H-D, hydrogen-deuterium; BPTI, bovine pancreatic trypsin inhibitor.

1.1 Introduction

Calcitonin (CT) is a single polypeptide hormone which consists of 32 amino acids with an N-terminal disulfide bridge between positions 1 and 7 and a C-terminal proline amide residue (Scheme 1-1). CT plays an important role in calcium-phosphorus metabolism (Copp et al., 1962; Kumar et al., 1963; Austin & Heath, 1981), and is used as treatment for various diseases, notably osteoporosis. However, human CT (hCT) easily associates and precipitates as insoluble fibrils upon storing in aqueous solution, which is a defect in therapeutic use. The understanding of the fibrillation process and of the hCT folding mechanism is expected to contribute to the further improvement of the long time stable aqueous therapeutic formulations of hCT (Arvinte & Ryman, 1992).

Early studies of the hCT association by electron microscopy revealed that it consists of fibrils of 80 Å in diameter, which often associate with one another (Sieber et al., 1970). Recently, Arvinte et al. (1993) studied the kinetics of hCT fibrillation by turbidity and electron microscopy measurements, and demonstrated that the fibrillation mechanism conforms to the double nucleation mechanism (Scheme 1-2) (Ferrone et al., 1980, 1985; Samuel et al., 1990).

The hCT fibrillation was also investigated by circular dichroism (CD), fluorescence and fourier transform infrared spectroscopy (FTIR) (Arvinte et al., 1993). These spectroscopic studies showed that hCT molecules form α-helical and intermolecular β-sheet secondary structure components, approximately 24 h after dissolving the peptide in aqueous solution. In the last few years structural analyses of CT have been carried out by the combined use of two-dimensional (2D) NMR and distance geometry algorithms. These studies indicated that a monomer CT molecule exhibits a well-defined α-helical conformation in the mixed

Scheme 1-1: Sequence of hCT

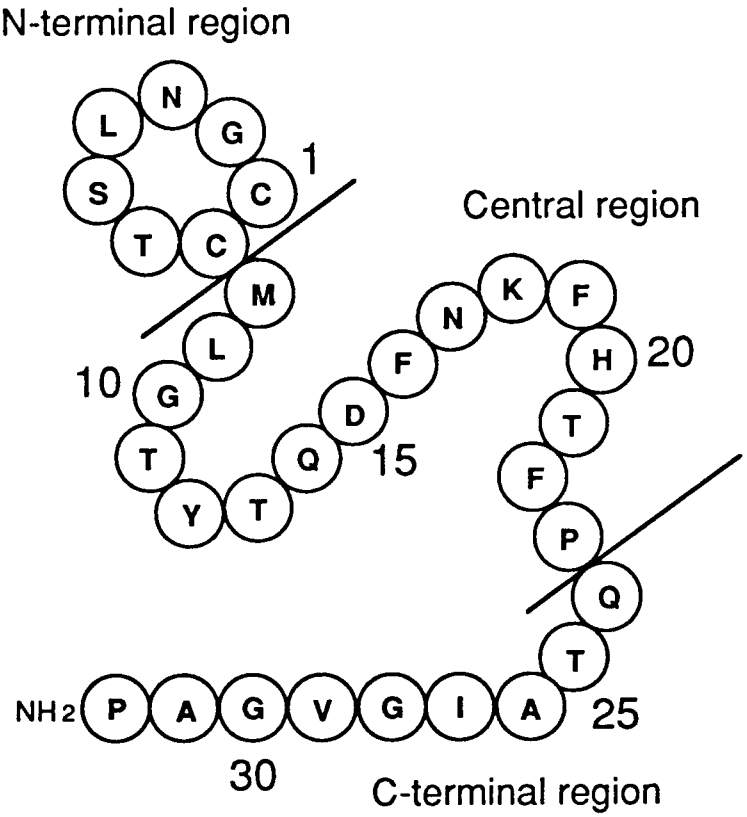

Scheme 1-2: Double nucleation mechanism

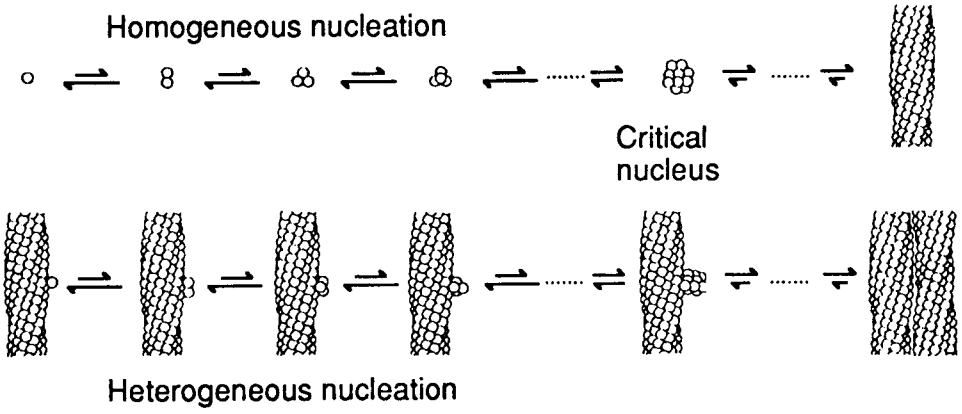

(Ferrone et al. (1985) *J.Mol.Biol. 183,* 611-631.)

solvents, but not in aqueous solution. For example, NMR studies of salmon CT (sCT) in TFE/H_2O (Meyer et al., 1991), MeOH/H_2O (Meadows et al., 1991) and SDS micelle (Motta et al., 1991a) showed that sCT forms an amphiphilic α-helical structure in the central region. For hCT, it has also been reported to adopt an α-helical structure in TFE/H_2O (Doi et al., 1990). It should be noted, however, that a short double-stranded antiparallel β-sheet structure was obtained in DMSO/H_2O (Motta et al., 1991b). Arvinte et al. (1993) assumed that the α-helix observed by CD in the process of the fibrillation coincides with the amphiphilic α-helix part elucidated by the NMR structural analyses.

The structural information of the fibrillation obtained by CD, fluorescence, and FTIR corresponds to that in the matured stage of the fibrillation. In the section 1.3.1, the initial stage of the fibrillation before the gelation could be investigated at atomic level by NMR spectroscopy. Recently, the mechanism of the peptide aggregation was extensively studied by NMR spectroscopy for various peptides (Zagorski & Barrow, 1992; Jarvis et al., 1994). However, few attempts have been made to observe the time-course of peptide peaks on aggregation or fibrillation on account of the rapid broadening and disappearance of the peptide peaks. We measured the time-course of aggregation process by 2D NMR method, demonstrating that the molecular association of hCT is initiated by the intermolecular hydrophobic interaction in the N-terminal and central regions, and that the C-terminal region is subsequently involved in the fibrillation.

It is noted that when hCT is dissolved in urea solution, no fibrillation was observed. It has been established that urea has an important function to play in influencing the solubility or aggregation behavior of protein molecules. The effects of urea on protein structure and protein-urea interaction have been investigated by X-ray crystallography (Pike &

Acharya, 1994) and NMR spectroscopy (Lumb & Dobson, 1992; Kim & Woodward, 1993; Liepinsh & Otting, 1994).

In order to investigate the influence of urea on the fibrillation behavior of hCT in aqueous urea media and how hCT fibrillation can be inhibited by the presence of urea, ^{1}H NMR spectra of hCT in aqueous urea solution were measured. On the other hand, caution must be preserved as carbamylation of the N-terminal amino group of hCT by urea is also found to occur, which substantially promotes the fibrillation process.

1.2 Materials and methods

Materials. Synthetic hCT was provided by Ciba-Geigy Pharmaceuticals, Basel, Switzerland. Powder of the hCT fibril (fhCT) was obtained by lyophilization of the aqueous solution of hCT (80 mg/mL) after storage at room temperature for 3 h. Urea was purchased from Nacalai Tesque (Kyoto, Japan).

Sample preparation for aqueous solution. The concentration of hCT was determined from its weight concentration. For resonance assignment in aqueous solution, the peptide was dissolved in 90% H_2O/10% D_2O (V/V) solution containing 0.015 M CD_3COOD (pH 2.9). The final concentration of peptide was 20 mg/mL (5.9 mM). It was confirmed that one-dimensional (1D) spectra did not change before and after 2D measurements at this concentration.

For time-course experiments, unless otherwise stated, the peptide was dissolved in 100% D_2O solution containing CD_3COOD (pH 2.9), and a series of spectra was recorded; the first spectrum was acquired about 6 min after dissolving the sample in D_2O. Since the fibrillation in the acidic condition proceeds more slowly as compared to the neutral condition, it was decided to use the former condition for this study. It was confirmed that the fibrillation of hCT in the acidic condition exhibits the same linearity of the logarithm of fibrillation time (t_f) and the logarithm of hCT concentration as that in the neutral condition (Arvinte et al., 1993). The value of t_f is the time corresponding to the intersection with the time axis of the linear increase in turbidity (Arvinte et al., 1993).

Sample preparation for urea solution. For resonance assignment in urea solution, the peptide was dissolved in a freshly prepared 90% H_2O/10% D_2O (V/V) solution containing urea and CD_3COOD (pH 2.9). The final concentration of peptide was 20 mg/mL (5.9 mM). For time

dependence experiments, the peptide was dissolved in 100% D_2O solution containing urea-d_4 and CD_3COOD (pH 2.9).

NMR measurements. All proton NMR spectra were recorded on a Bruker AMX600 spectrometer at 300 K. For resonance assignments, DQFCOSY (Piantini et al., 1982; Rance et al., 1983), HOHAHA (Braunschweiler & Ernst, 1983; Davis & Bax, 1985) and NOESY (Jeener et al., 1979; Macura et al., 1981) were run according to the time-proportional phase incrementation method (TPPI) (Marion & Wüthrich, 1983). NOESY spectra were recorded with mixing time of 300 ms, and HOHAHA experiments were acquired with mixing times of 40 and 80 ms. FELIX (Biosym inc.) was used for data processing and signal assignment on a Silicon Graphics workstation.

For rapid 2D measurements, HOHAHA (mixing time 40 and 80 ms) and ROESY (Bax & Davis, 1985) (mixing time 100 and 200 ms) data were collected by the states-TPPI method (Marion et al., 1989) without phase cycling. Applying this method, it took about 5 min to measure 256(t1) x 512(t2) data matrix. Shifted sine bell squared weight functions were applied in both dimensions and the data were zero filled to a final size of 1K x 1K.

1.3 Results

1.3.1 Fibrillation of hCT in aqueous solution

Sequential signal assignment of hCT in aqueous solution. The signal assignment of the hCT spectrum was completed according to the well-established sequential approach (Billeter et al., 1982; Wüthrich et al., 1982). The assignment of the resonance are summarized in Table 1-1. The NH-α fingerprint region of the HOHAHA spectrum at 300 K with 40 ms mixing time showed all expected cross peaks except for Cys^1, Pro^{23}, and Pro^{32} (Figure 1-1). Some additional peaks were observed in the same region, which can be explained by the presence of *cis-trans* isomers of the prolyl residues. The existence of the isomers of the prolyl residues was reported in DMSO and DMSO/H_2O solution (Motta et al., 1991b) as well as in aqueous solution recently (Kern et al., 1993).

Concentration and time dependence of NMR spectra of hCT in aqueous solution. 1D ^1H NMR spectra of hCT were measured at various concentrations (1, 5, 10, 20, and 80 mg/mL) in 100% D_2O solutions. All spectra were obtained about 6 min after dissolution. There were little differences observed in the chemical shift values and the line widths of nonlabile protons in all the recorded spectra. Some peaks at the concentration of 80 mg/mL shifted slightly (< 0.02 ppm), as compared with those at lower concentrations (1-20 mg/mL). Peak intensities increased linearly with an increase of the concentration, as was expected. These results indicate that just after dissolution (6 min), most of hCT molecules exist as a monomer even at high concentration (80 mg/mL) in aqueous solution.

After 6 min, the spectra of hCT at lower concentrations (1-20 mg/mL) showed little broadening of the line widths without chemical shift change,

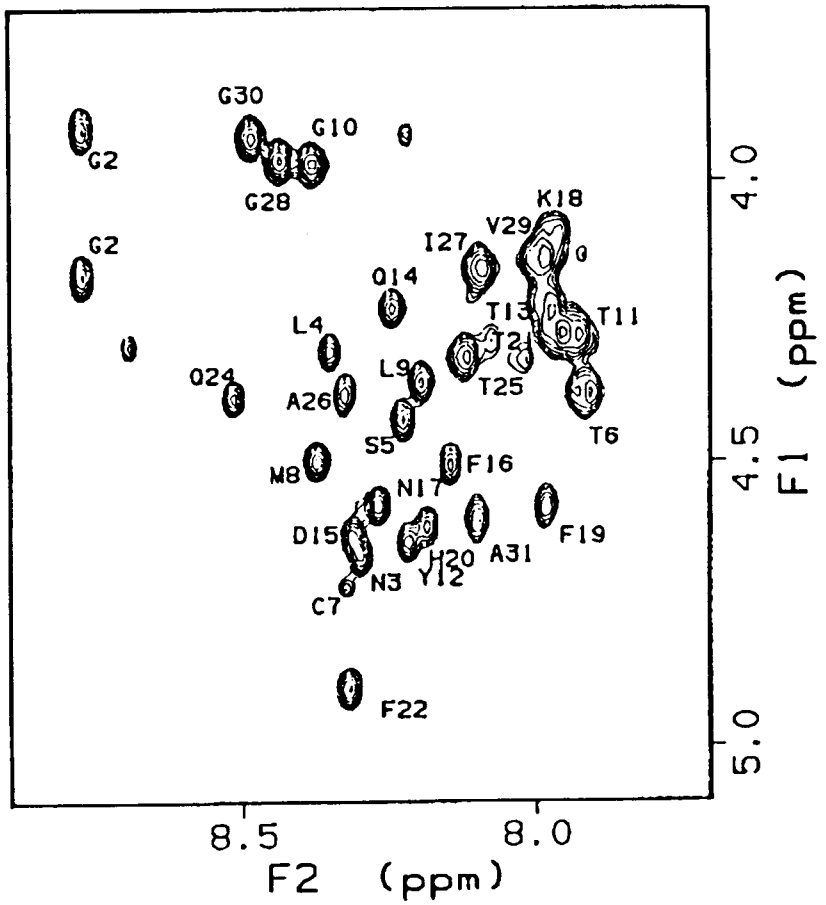

Figure 1-1: Backbone fingerprint region of the HOHAHA (40 ms) spectrum of hCT in 90% H_2O/ 10% D_2O (pH 2.9) at 300 K. Cross peaks are labeled with their amino acid residue name (single letter code) and sequence numbers.

Table 1-1: ^{1}H assignment and chemical shift data for hCT (20 mg/ml) in aqueous solution, pH 2.9, 300 K

residue		NH	Hα	Hβ	others
1	Cys		4.35	3.26, 3.36	
2	Gly	8.77	3.91, 4.17		
3	Asn	8.30	4.66	2.83, 2.92	δNH2 6.96, 7.63
4	Leu	8.35	4.31	1.77	γC H 1.65,
					δCH3 0.88, 0.93
5	Ser	8.22	4.42	3.91	
6	Thr	7.91	4.38	4.31	γCH3 1.21
7	Cys	8.32	4.72	3.15, 3.26	
8	Met	8.37	4.50	2.03, 2.10	γCH2 2.52, 2.60
					εCH3 2.06
9	Leu	8.19	4.36	1.61	γC H 1.68,
					δCH3 0.88, 0.93
10	Gly	8.38	3.97		
11	Thr	7.94	4.27	4.13	γCH3 1.11
12	Tyr	8.21	4.64	2.99, 3.09	2,6H 7.10, 3,5H 6.79
13	Thr	7.98	4.22	4.16	γCH3 1.16
14	Gln	8.24	4.22	1.91, 1.98	γCH2 2.28
					εNH2 6.85, 7.47
15	Asp	8.31	4.64	2.73, 2.82	
16	Phe	8.14	4.50	3.03, 3.13	2,6H 7.21, 3,5H 7.30
					4H 7.27
17	Asn	8.26	4.58	2.71, 2.76	δNH2 6.93, 7.57
18	Lys	7.96	4.09	1.58	γCH2 1.57, δCH2 1.24
					εCH2 2.90, NH2 7.51
19	Phe	7.98	4.58	2.92, 3.13	2,6H 7.23, 3,5H 7.32
					4H 7.27
20	His	8.18	4.62	3.05, 3.16	2H 8.51, 4H 7.09
21	Thr	7.97	4.27	4.08	γCH3 1.10
22	Phe	8.31	4.90	2.92, 3.17	2,6H 7.30, 3,5H 7.33
					4H 7.30
23	Pro		4.44	1.93, 2.28	γCH2 1.99
					δCH2 3.59, 3.81
24	Gln	8.51	4.39	2.01, 2.13	γCH2 2.40
					εNH2 6.84, 7.55
25	Thr	8.12	4.32	4.21	γCH3 1.22
26	Ala	8.32	4.38	1.37	
27	Ile	8.09	4.16	1.86	γCH2 1.19, 1.49
					γCH3 0.91, δCH3 0.84
28	Gly	8.44	3.96		
29	Val	7.99	4.14	2.15	γCH3 0.90, 1.00
30	Gly	8.48	3.92		
31	Ala	8.10	4.60	1.35	
32	Pro		4.39	1.93, 2.29	γCH2 2.01
					δCH2 3.66, 3.78
					NH2 6.98, 7.61

and no spectral change was observed over 24 h (data not shown). At these low concentrations, the fibrillation would proceed very slowly; therefore, we refer to this condition (20 mg/mL) as the monomer condition.

On the other hand, after 6 min, 1D ^1H NMR signals of hCT at 80 mg/mL started to show a gradual broadening, but were not accompanied either by any change of chemical shift or by the appearance of new peaks. Around 60 min, a drastic change in the spectra occurred, whereby most of the peptide peaks disappeared (Figure 1-2). Figure 1-3 shows the relative intensities of the peptide peaks as a function of time. The change in the NMR spectra at 60 min may be attributed to a transient phase change from particles to a hard, turbid gel. The value of t_f in the acidic condition was estimated to be 40 min by the NMR results, which is equal to the value obtained by absorption measurement (Arvinte et al., 1993). Hereafter, we refer to this condition (80 mg/mL) as the fibril condition.

The water resonance shifted to the downfield, and broadened after the change in the peptide peaks at 60 min. This phenomenon suggests the formation of a hydrogen bond network among water molecules leading to the gelation of the solution, and subsequent increase in the viscosity.

It should be noted that some peaks in the 1D spectrum remained even at 70 min, whereas the others disappeared completely. This means that all the peaks did not broaden and disappear simultaneously in the course of the fibrillation.

Time-course of 2D NMR spectra of hCT in the fibril condition. Details of the signal broadening in the fibril condition in D_2O were further investigated for each residue by 2D NMR spectroscopy. 2D HOHAHA spectrum in the fibril condition which was acquired for 7-13 min after dissolution was almost identical to the spectrum used for the resonance assignment. During following 30 min, cross peaks broadened gradually,

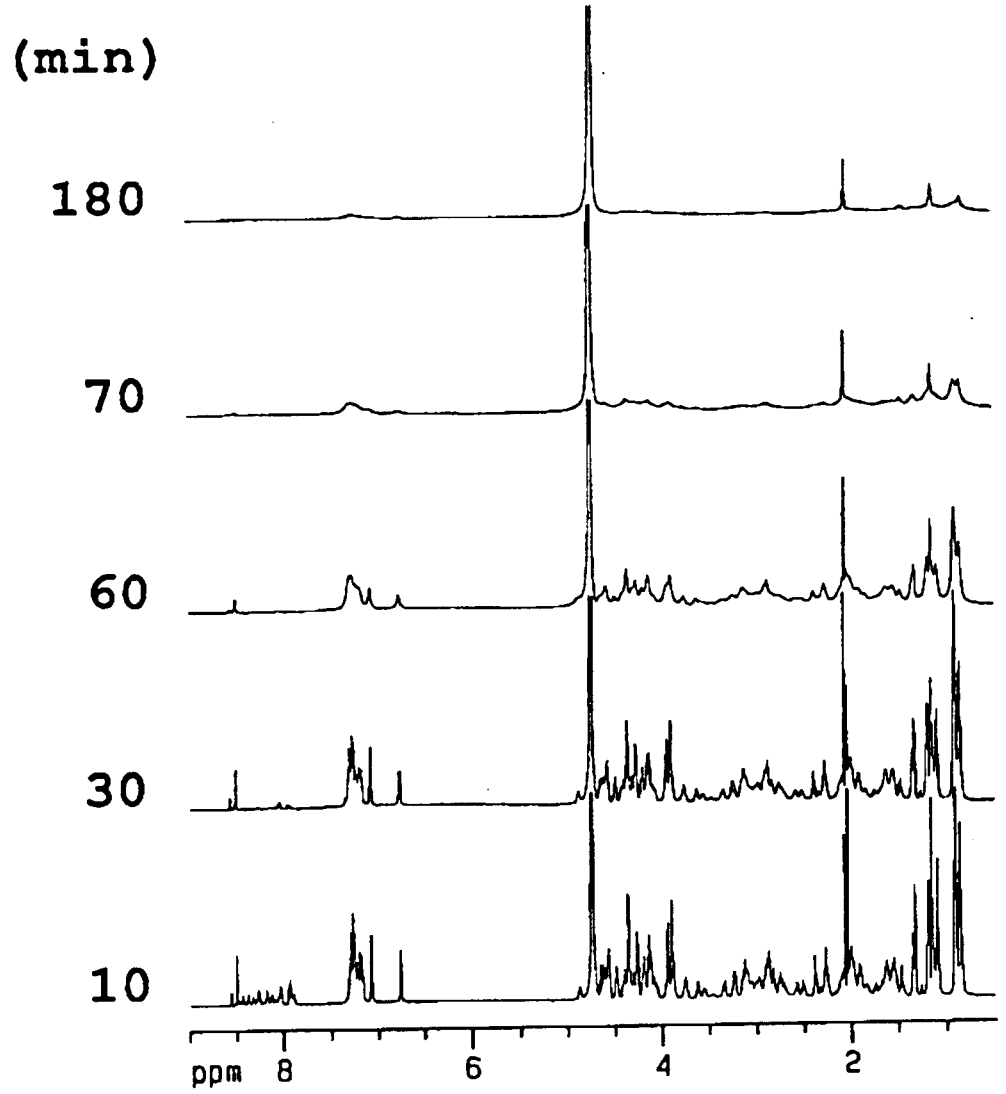

Figure 1-2: Time-course of the ^{1}H NMR spectra of hCT in the fibril condition (80 mg/ml, pH 2.9, 300 K).

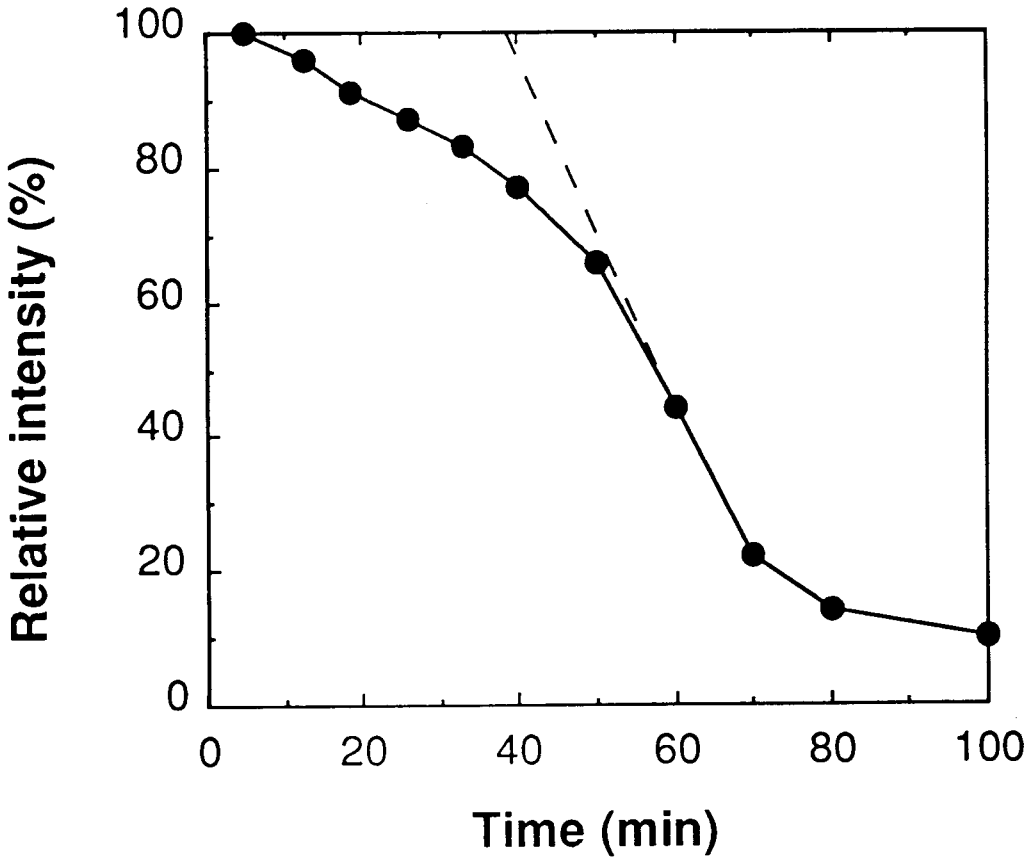

Figure 1-3: Change in time of the averaged intensity of hCT peaks in the 1D ^{1}H NMR spectra in the fibril condition. The averaged relative peak heights of resolved nonexchangeable protons are plotted.

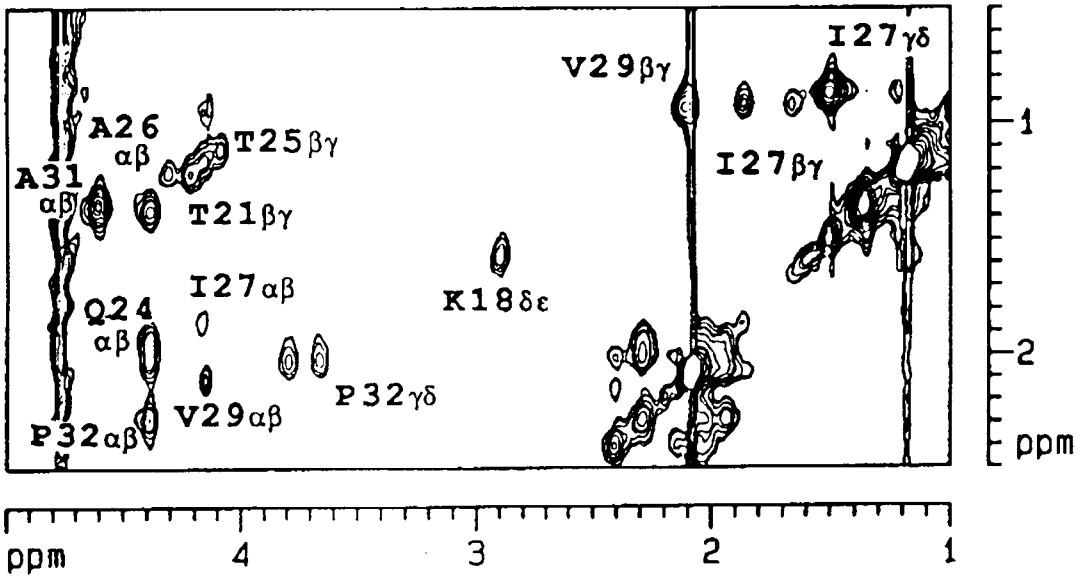

Figure 1-4: Time-course of the aliphatic region of the HOHAHA (40 ms) spectra of hCT in the fibril condition after dissolution for 71-75 min. Cross peaks are labeled with their amino acid residue name (single letter code) and sequence numbers.

and their intensities became smaller, in accordance with 1D spectra. Figure 1-4 shows the aliphatic region of the 2D HOHAHA spectrum obtained during 70-76 min period, when the significant change occurred in the time-course of the 1D spectra. Almost all remaining cross peaks in the spectrum corresponded to residues located in the C-terminal region, whereas all peaks of residues in the N-terminal and central regions disappeared. In exception, some side-chain cross peaks (δ-ε of Tyr^{12}, δ-ε of Lys^{18} and β-γ of Thr^{21}) in those regions did not disappear.

Time-course of 1D and 2D HOHAHA spectra in 90% H_2O/10% D_2O in the fibril condition was also conducted in order to examine changes of NH-α cross peaks in the fibril condition. The chemical shifts of some NH-α cross peaks in the fibril condition were slightly different from those in the monomer condition (Figure 1-5a). All the cross peaks broadened a little with time (Figure 1-5b), and then, the cross peaks of residues in the N-terminal and central regions broadened and disappeared 40 min after dissolution, but those in the C-terminal region remained (Figure 1-5c). This broadening feature of the NH-α peaks was identical to that of the cross peaks of aliphatic protons, however, the NH-α peaks disappeared faster than the aliphatic cross peaks (Figure 1-5d).

ROESY spectra instead of NOESY spectra were measured to obtain spatial information about the fibrillation mechanism since NOESY experiments without phase cycling gave rise to artifacts. The time-course of ROESY spectra collection was every 6 min after dissolution, and example spectra (7-13 and 41-47 min after dissolution) are shown in Figure 1-6a and b, respectively. ROESY spectra (mixing time 100 and 200 ms) which were recorded during the fibril formation provided intra-residue and sequential NOEs. Neither long range NOEs nor chemical exchange peaks were observed for both mixing times. The α-β intra-residue NOE cross peaks of the C-terminal region ($Ala^{26,31}$, Ile^{27},

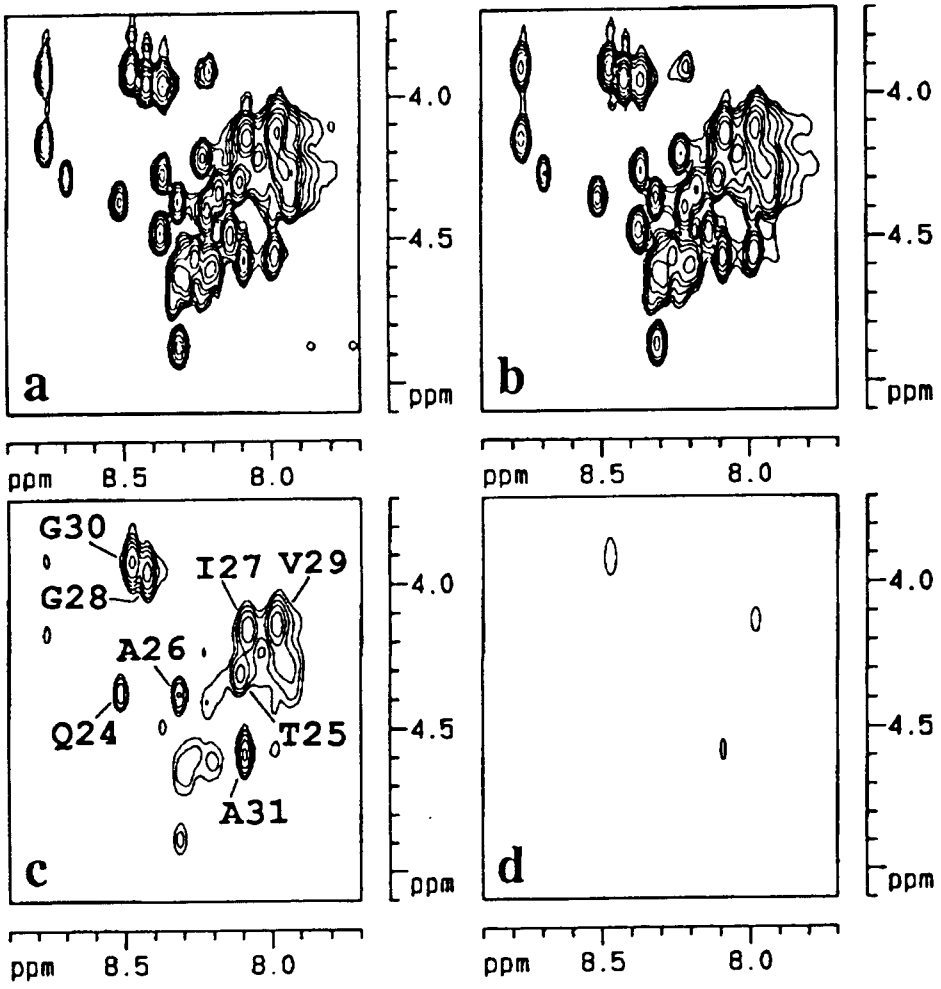

Figure 1-5: Time-course of the fingerprint region of the HOHAHA (40 ms) spectra of hCT in the fibril condition after dissolving hCT in 90% H_2O/10% D_2O, for 7-13 min (a), 30-36 min (b), 44-50 min (c), and 52 -58 min (d). Cross peaks are labeled with their amino acid residue name (single letter code) and sequence numbers.

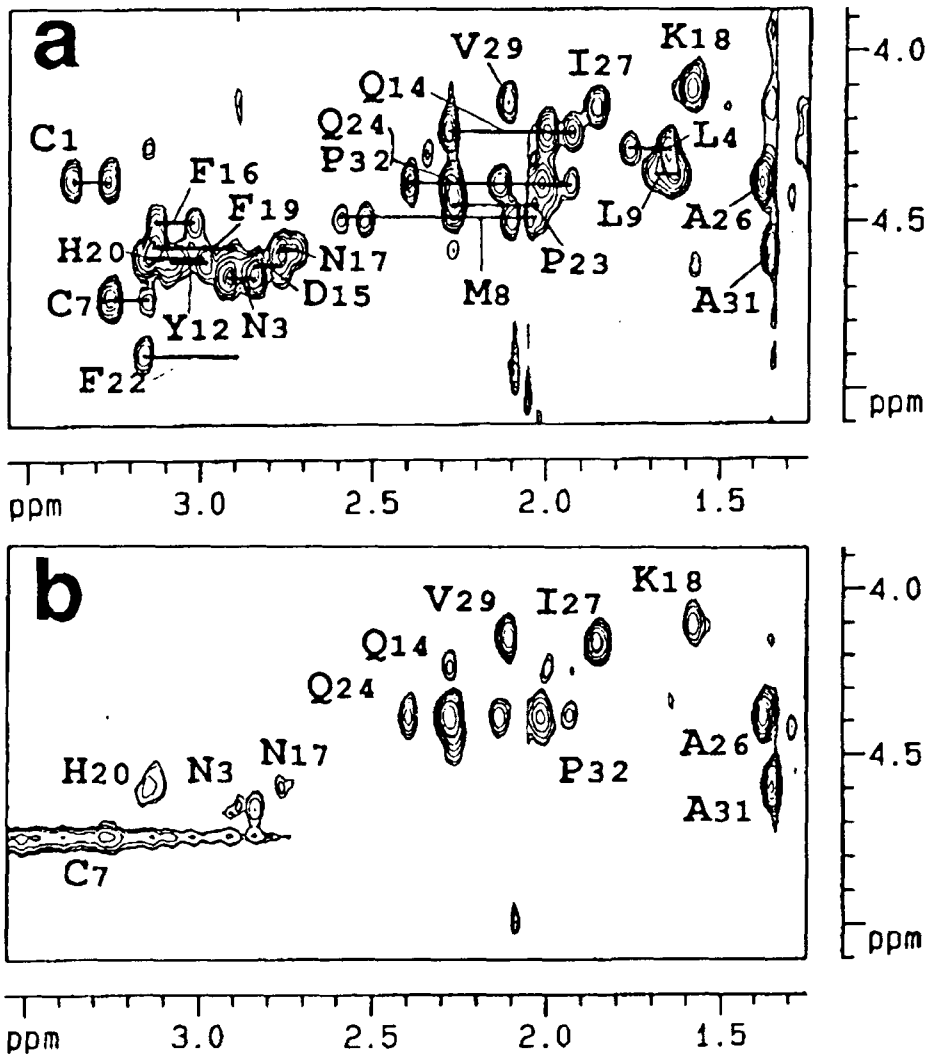

Figure 1-6: The aliphatic region of the ROESY (200 ms) spectra of hCT in the fibril condition after dissolution for 7-13 min (a) and 41-47 min (b).

Val^{29}, and Pro^{32}) are scarcely changed between Figure 1-6a and b. As for the N-terminal and central residues, the cross peaks of Cys^{1}, $Leu^{4,9}$, Met^{8}, Tyr^{12}, Asp^{15}, and $Phe^{16,19,22}$ (Group A) disappeared, but the peaks of $Asn^{3,17}$, Cys^{7}, Gln^{14}, Lys^{18}, and His^{20} (Group B) remained weak. The α-β cross peak of Ser^{5} also remained weak in the same ROESY spectrum (data not shown), but the signal change of threonine residues were not clearly observed because of overlapped artifacts near diagonal peaks. These were the cases for both ROESY spectra of mixing time 100 and 200 ms.

Hydrogen-deuterium (H-D) exchange experiments. Generally speaking, H-D exchange experiments of amide protons offer information about hydrogen bonding derived from secondary structure and solvent accessibility to the peptide backbone. Figure 1-7 displays the 1D spectra of NH proton regions for the fibril (a) and monomer (b) conditions, respectively. The spectra of the monomer condition remained unchanged, except for the labile NH protons, for the first 3 h. The two sharp, unaltered peaks at 8.51 and 8.57 ppm are the C_2 protons of His^{20} in the *trans* and *cis* isomers, respectively (Kern et al., 1993).

The 1D spectra at 6, 12, and 24 min in the fibril and monomer conditions show that NH peaks in the fibril condition disappeared slower than those in the monomer condition, despite broadening of the peaks by the fibrillation in the fibril condition. The anomalous behavior in the signal disappearance between the fibril and monomer conditions can be attributed to differences in their respective H-D exchange rates. Namely, the H-D exchange would proceed more slowly in the fibril condition compared to the monomer condition. Almost all the NH protons exchanged with D_2O for a period of 50 min after dissolution.

In order to study specific details of the H-D exchange of the NH protons, time-course of 2D HOHAHA spectra were measured for the

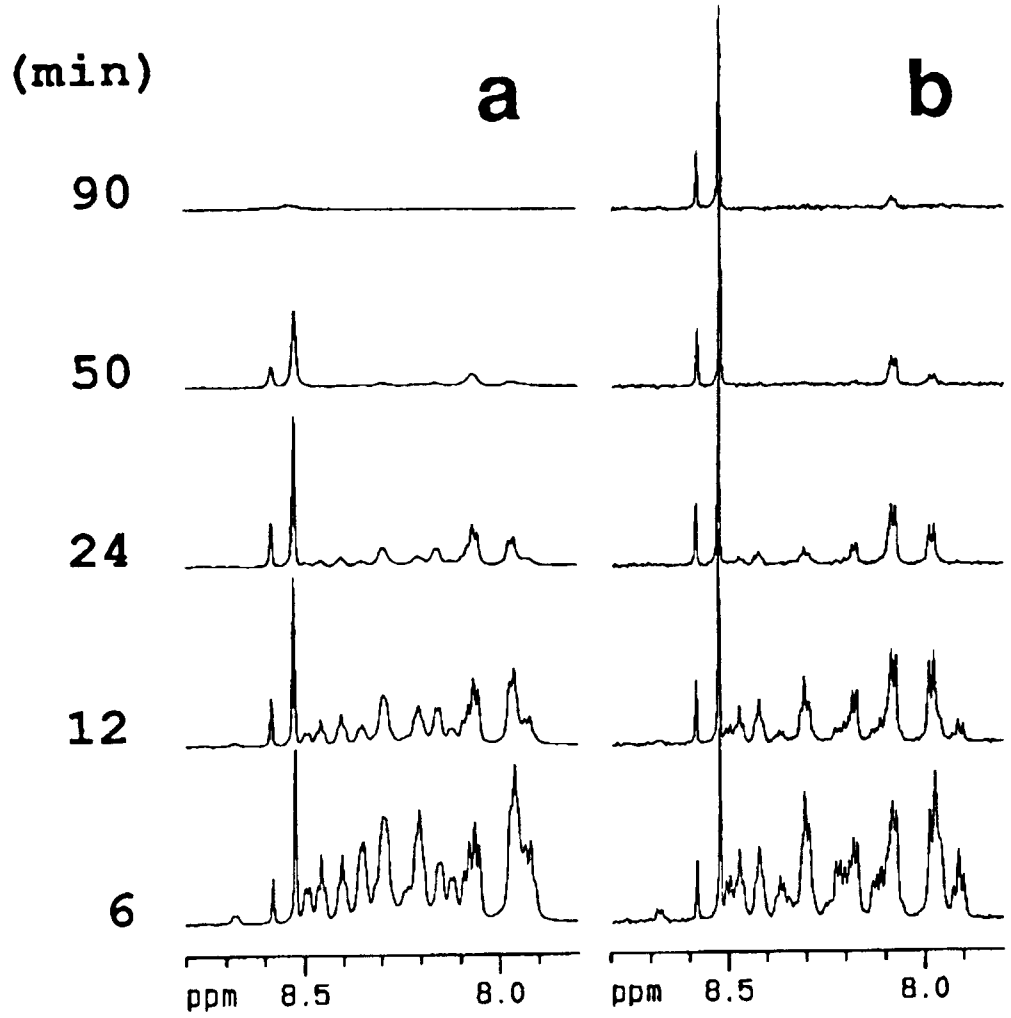

Figure 1-7: Time-course of the NH signals of hCT in the fibril condition (a) and in the monomer condition (b).

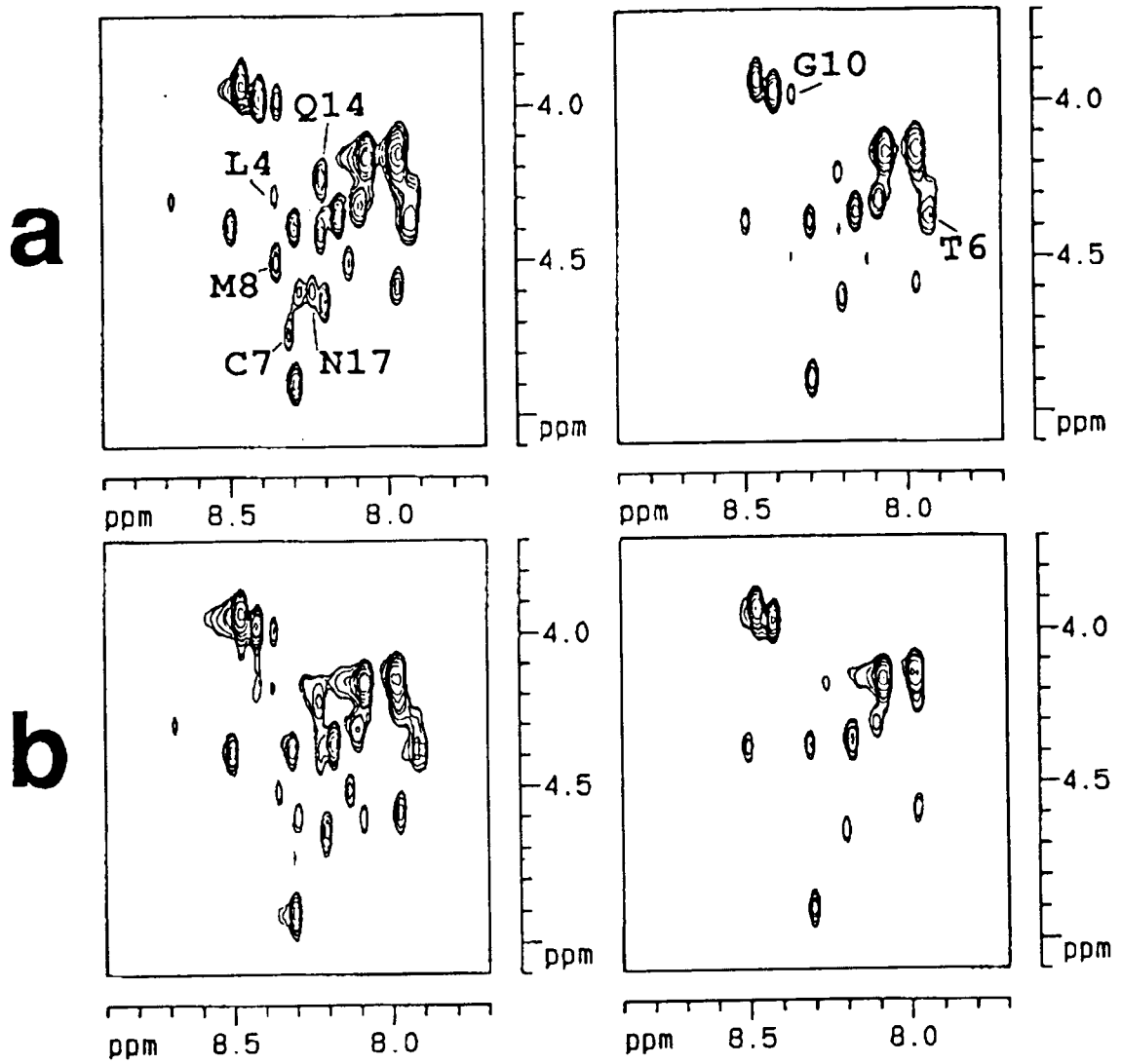

Figure 1-8: Time-course of the fingerprint region of the HOHAHA (40 ms) spectra of hCT in the fibril (a) and monomer (b) condition for 7-13 min (left), and 13-19 min (right) after dissolution. Labels with their amino acid residue name (single letter code) and sequence number indicate cross peaks whose H-D exchange rates in the fibril condition are slower than those in the monomer condition.

both conditions after dissolution. Some cross peaks (Leu^4, Thr^6, Cys^7, Met^8, Gly^{10}, Gln^{14}, and Asn^{17}) disappeared significantly slower in the fibril condition (upper in Figure 1-8) than those in the monomer condition (lower in Figure 1-8). All these residues are located in the N-terminal and central regions. Thus, the H-D exchange rates of these residues in the fibril condition would be slower than those in the monomer condition. There was no discernible difference in the H-D exchange rates of the C-terminal residues between the fibril and monomer condition.

1.3.2 Characterization of fhCT and its fibrillation in aqueous solution

1D ^1H NMR spectra of fhCT in D_2O were also measured at various concentrations (1-80 mg/mL). As stated above, NMR signals of the hCT fibrils were considered to be too broad to observe. However, as shown in Figure 1-9, 6 min after the dissolution of fhCT in D_2O, it afforded broad signals, whose chemical shifts were identical to those of hCT. The line widths became broader with increasing the concentration. At higher concentrations (> 40 mg/mL) the peptide precipitated, and the solution promptly became gel.

1D and 2D HOHAHA (mixing time 40 ms) spectra of the peptide in the fhCT solution (40 mg/mL) showed a signal broadening within 1 h, while the signal broadening in the hCT solution at the same concentration of 40 mg/mL did not occur even 24 h after the dissolution. However, the signal broadening feature observed in the fhCT solution appeared to be similar to that of the hCT solution, indicating that the peaks in the N-terminal and central regions disappeared faster than those in the C-terminal region (Figure 1-10). These results suggest that a part of the fibrils dissociate to

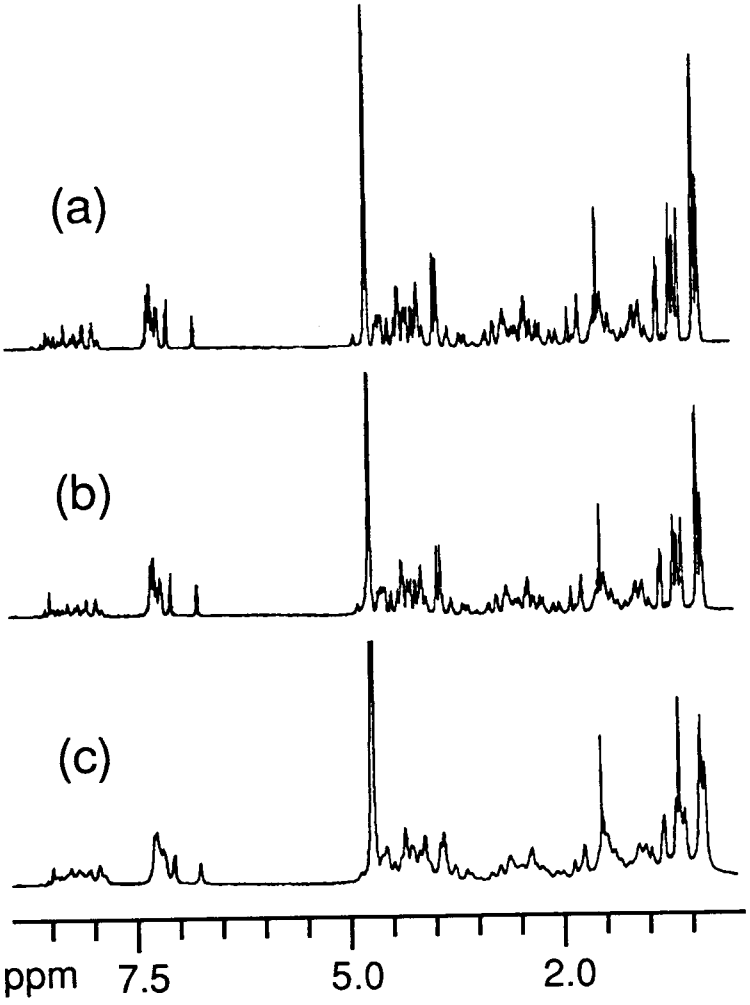

Figure 1-9: ^1H NMR spectra of hCT (10 mg/mL) (a), fhCT (10 mg/mL) (b), and fhCT (40 mg/mL) (c), all in D_2O at 300 K, pH 2.9.

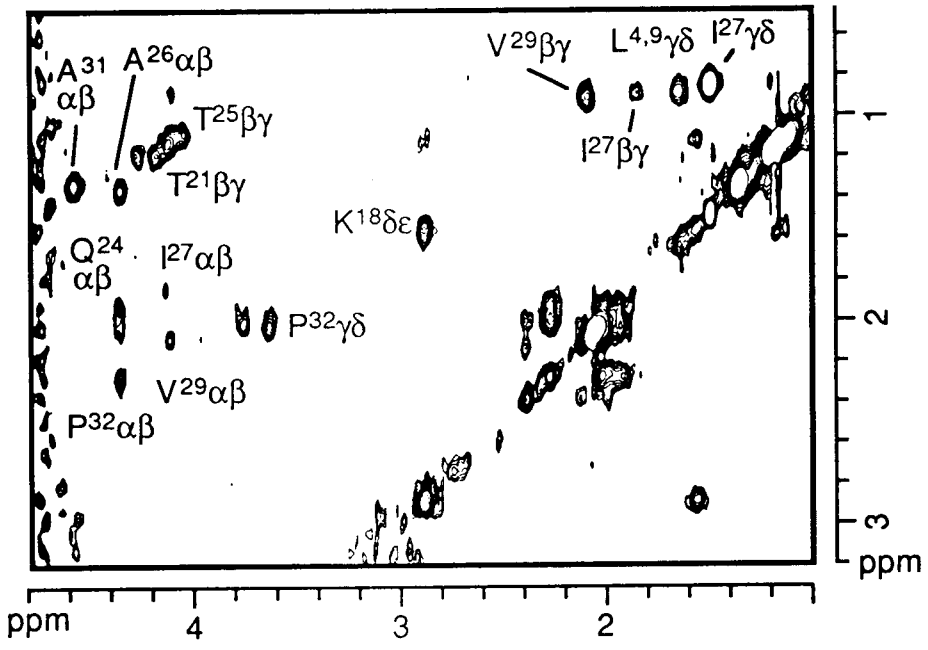

Figure 1-10: 2D HOHAHA spectrum (mixing time 40 ms) of fhCT (40 mg/mL) after the dissolving the peptide in D2O for 27-32 min, at 300 K, pH 2. 9. Cross peaks are labeled with their amino acid residue name (single letter code) and sequence numbers.

monomer molecules by lyophilization, thereby providing observable NMR signals of the peptide. The small amount of the tightly associated fibril molecules in the fhCT solution would act as a core, forcing the dissociated monomer molecules to reassociate very rapidly in the same way as that of the hCT fibrillation process.

When a small amount of fhCT (10% wt) was added to the hCT solution (total concentration 20 mg/mL), the peaks became broader within several hours, comparable to the 100% fhCT solution at the same concentration (20 mg/mL). This fact also serves to suggest that fhCT promotes the association of the peptide molecules.

1.3.3 Fibrillation of hCT in urea solution

Time-course of ^1H NMR spectra of hCT and fhCT in urea solution. Time course of ^1H NMR spectra of hCT (80 mg/mL) in a freshly prepared urea solution showed no change in the peptide signals over 24 h, in terms of both chemical shift and appearance of new peaks. Conversely, in the absence of urea, all the peptide signals were significantly broadened within 1 h under identical conditions (Figure 1-1). Figure 1-11 shows the time dependence of the peak intensities for aqueous solutions of hCT in the presence and absence of urea. When fhCT was dissolved in a freshly prepared 6 M urea solution, the signals were sharp and identical to those of hCT in the urea solution, and the spectra showed no significant change over 24 h as well as hCT. Thus, the association of hCT molecules is prevented by urea, and the fibril core is considered to dissociate to the monomer in the highly concentrated urea solution. From the above findings, it can be readily concluded that urea actively functions in preventing the fibrillation of hCT. However, careful examination of the time dependence behavior of peak intensities revealed

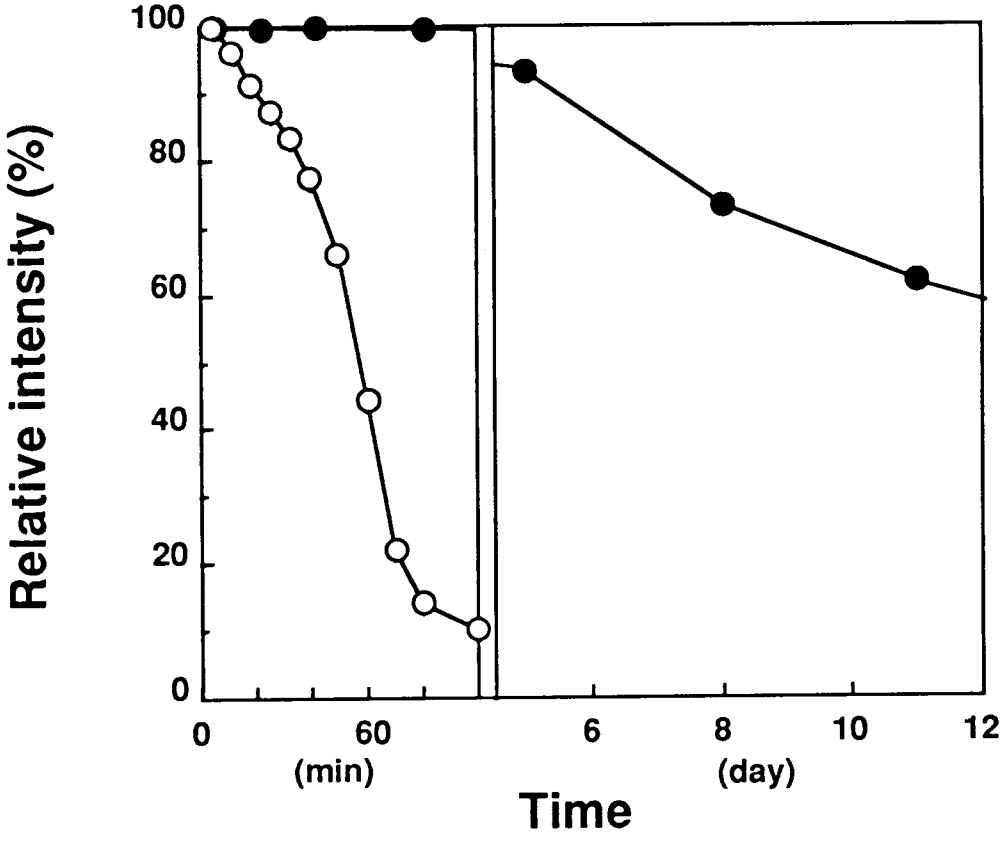

Figure 1-11: Time dependence of peak intensities of hCT in the absence of urea (open circle) and in the presence of 6 M urea (closed circle). Other conditions; hCT concentration 80 mg/mL, temperature 300 K, pH 2. 9 were the same for both of the solutions.

that urea does not completely inhibit fibrillation, as the process continues to occur, albeit at a much reduced rate. The reasons for this behavior will be addressed later in the 1.3.4.

Sequential signal assignment of hCT in urea solution. Assignments of the hCT signals in urea solution were performed by using the sequential approach (Billeter et al., 1982; Wüthrich et al., 1982) as above-mentioned in 1.3.1. Figure 1-12 displays the NH-α fingerprint region of the HOHAHA spectrum of hCT in the urea solution, and yields all the expected cross peaks except for Cys^{1}, Pro^{23}, and Pro^{32}. The ratio of the isomers of the prolyl residues in the absence of urea is 67, 25, and 8% for (*trans, trans*)-, (*cis, trans*)-, and (*trans, cis*)-(Pro^{23}, Pro^{32}) conformers, respectively (Kern et al., 1993), whereas in urea solution, the ratio was changed to 75, 16, and 9% for these three conformers. The assignment of the resonance are summarized in Table 1-2.

Comparison of amide and Cα proton chemical shifts of hCT in the absence and presence of urea. Compared to the chemical shift values of hCT in aqueous solution (Table 1-1), all nonlabile protons of side chains showed only very small chemical shift change (≤ 0.02 ppm) with urea concentrations up to 8 M. This suggests that conformational details of the amino acid side chains appear to be preserved in the presence of urea. On the other hand, resonances of the amide protons were significantly shifted downfield (solid bars in Figure 1-13). The magnitudes of the downfield shifts were large in the N-terminal and central regions, whereas those in the C-terminal region were small. Hence, the environment around the N-terminal and central regions changes significantly through interactions with urea molecules. The maximum observed shift was 0.2 ppm for the amide proton of His^{20}, and the average value was 0.07 ppm, which was almost equivalent to that observed in bovine pancreatic trypsin inhibitor

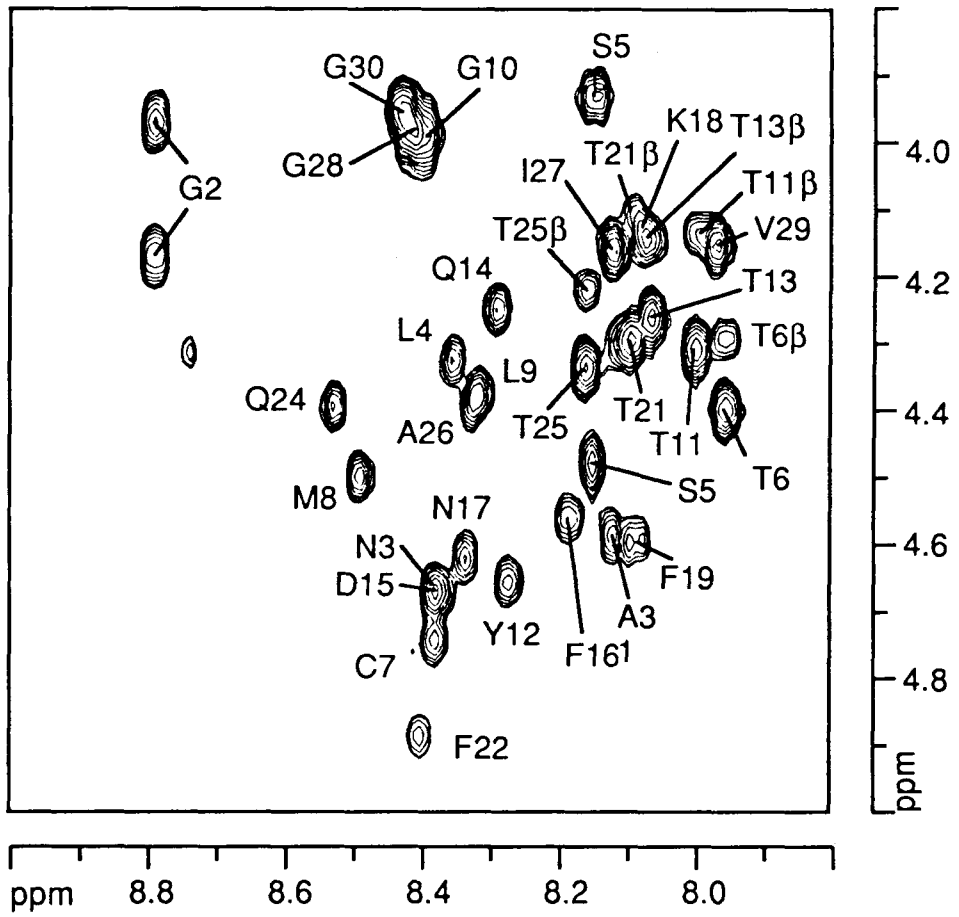

Figure 1-12: Backbone fingerprint region of the HOHAHA (80 ms) of hCT in a freshly prepared 6 M urea 90% H_2O/10% D_2O (pH 2.9) solution at 300 K. All cross peaks are labeled with their amino acid residue name (single letter code) and sequence numbers. A table of chemical shift of hCT in 6 M urea is available as supplementary material.

Table 1-2: ^{1}H assignment and chemical shift data for hCT (20 mg/ml) in 6 M urea solution, pH 2.9, 300 K

residue	NH	Hα	Hβ	others
1 Cys		4.33	3.27, 3.34	
2 Gly	8.80	3.97, 4.17		
3 Asn	8.39	4.68	2.83, 2.90	δNH2 6.98, 7.50
4 Leu	8.37	4.33	1.75	γCH 1.65, δCH3 0.88, 0.92
5 Ser	8.16	4.48	3.93	
6 Thr	7.97	4.40	4.30	γCH3 1.20
7 Cys	8.39	4.75	3.13, 3.28	
8 Met	8.50	4.50	2.01, 2.09	γCH2 2.52, 2.59 εCH3 2.06
9 Leu	8.33	4.38	1.62	γCH 1.67, δCH3 0.88, 0.93
10 Gly	8.40	3.93		
11 Thr	8.07	4.31	4.14	γCH3 1.12
12 Tyr	8.28	4.66	2.96, 3.09	2,6H 7.10, 3,5H 6.79
13 Thr	8.07	4.27	4.14	γCH3 1.14
14 Gln	8.30	4.26	1.89, 1.93	γCH2 2.27 εNH2 6.88, 7.41
15 Asp	8.39	4.68	2.76, 2.83	
16 Phe	8.19	4.57	3.00, 3.13	2,6H 7.21, 3,5H 7.30 4H 7.27
17 Asn	8.35	4.63	2.70, 2.74	δNH2 7.01, 7.56
18 Lys	8.09	4.15	1.59	γCH2 1.56, δCH2 1.13 εCH2 2.89, NH2 7.55
19 Phe	8.10	4.60	2.93, 3.12	2,6H 7.23, 3,5H 7.32 4H 7.27
20 His	8.38	4.68	3.07, 3.16	2H 8.51, 4H 7.07
21 Thr	8.11	4.30	4.10	γCH3 1.10
22 Phe	8.41	4.89	2.92, 3.18	2,6H 7.30, 3,5H 7.33 4H 7.30
23 Pro		4.46	1.94, 2.28	γCH2 2.00 δCH2 3.60, 3.82
24 Gln	8.54	4.40	2.01, 2.13	γCH2 2.41 εNH2 6.89, 7.41
25 Thr	8.17	4.34	4.23	γCH3 1.22
26 Ala	8.33	4.40	1.37	
27 Ile	8.13	4.16	1.84	γCH2 1.18, 1.49 γCH3 0.91, δCH3 0.86
28 Gly	8.43	3.98		
29 Val	7.98	4.16	2.10	γCH3 0.92
30 Gly	8.44	3.95		
31 Ala	8.13	4.59	1.34	
32 Pro		4.38	1.94, 2.28	γCH2 2.03 δCH2 3.65, 3.79 NH2 7.00, 7.61

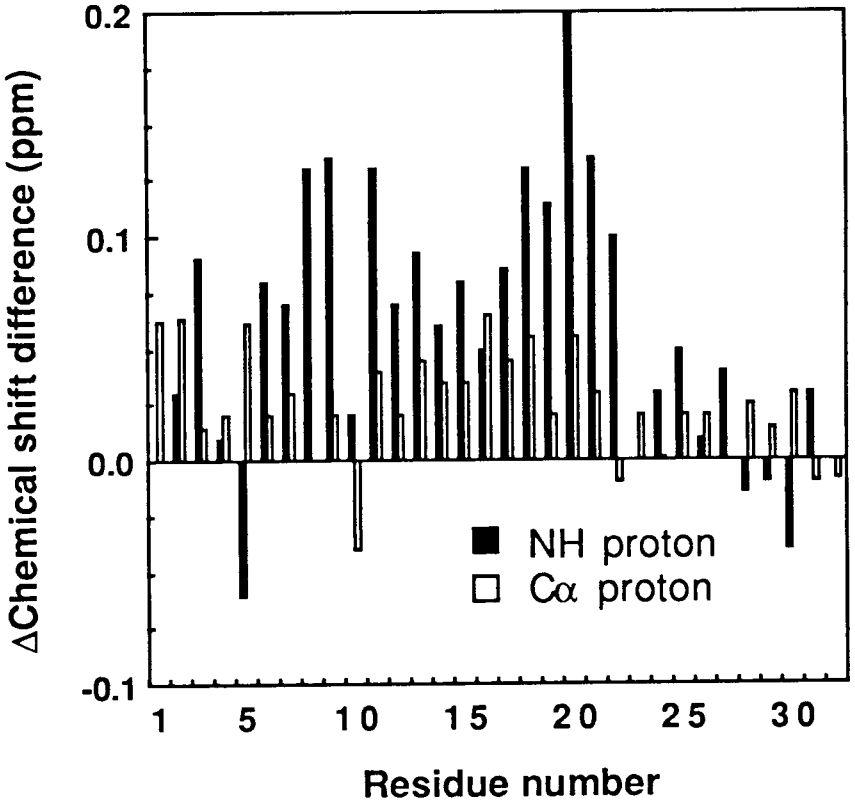

Figure 1-13: Differences in the chemical shifts of the NH (solid bars) and Cα (open bars) protons of hCT in freshly prepared 6 M urea solution at 300 K and pH 2.9, from the values in aqueous solution under the same conditions.

(BPTI) and the acidic protein PEC-60 in urea solutions (Liepinsh & Otting, 1994).

The chemical shifts of the Cα protons also showed downfield shifts in urea solution, although the magnitude of the shifts were smaller than those of the NH protons (open bars in Figure 1-13).

1.3.4 Effect of carbamylation at the N-terminus of hCT on the fibrillation in urea solution

Carbamylation at an N-terminal amino group of hCT in urea solution. As shown in Figure 1-11, the peak intensities of hCT show a gradual decrease, indicating that fibrillation occurs even in the urea solution, despite the fact that urea can prevent fibrillation. After the hCT urea solution (40 mg/mL) was heated up for 15 min at 343 K, 1D and 2D ^{1}H NMR spectra were measured at 300 K and pH 2.9. As a consequence, all peptide peaks broadened significantly within 1 h, accompanied by gelation of the solution. Furthermore, besides the original peaks of hCT in urea solution before heating, new NH-Cα cross peaks appeared. The proportion of the new peaks to the corresponding original peak depends on the heating time at 343 K. It was also confirmed that there was no chemical exchange between the original and new peaks by changing temperature and pH. Some of the new NH protons (Gly^2, Leu^4, Ser^5, and Thr^6) shifted more than 0.2 ppm, as compared to the original peaks (Figure 1-14a).

An explanation for the above phenomenon can be seen from the below scheme (Stark et al., 1960), where urea breaks down to form the cyanate, which in turn reacts with the α-amino group to form carbamyl derivatives.

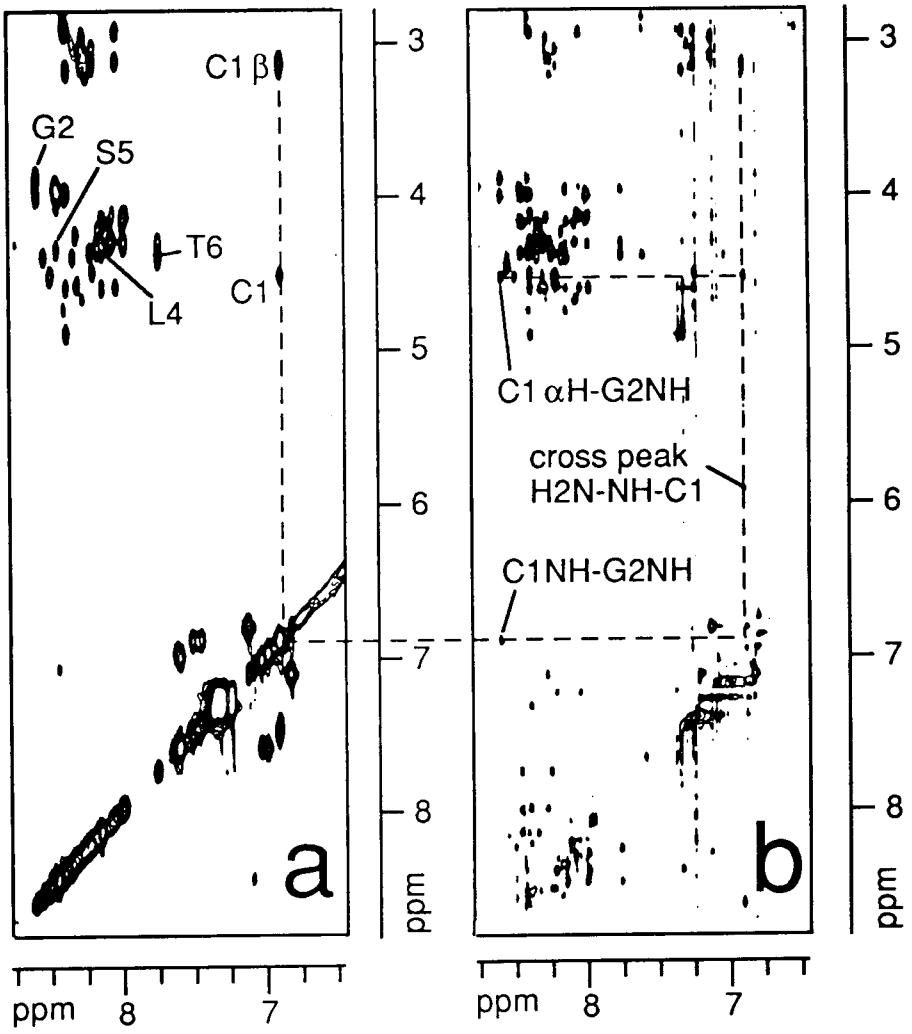

Figure 1-14: HOHAHA (80 ms) (a) and ROESY (200 ms) (b) spectra of carbamylated hCT in 6 M urea solution at 300 K. Some cross peaks which were mentioned in the text are labeled with their amino acid residue name (single letter code) and sequence number. A table of chemical shift of carbamylated hCT in 6 M urea is available as supplementary material.

$H_2NCONH_2 \longrightarrow CNO^- + NH_4^+$

$CNO^- + H_3N^+$-peptide $\longrightarrow H_2NCONH$-peptide

It would also follow that the α-amino group of N-terminus and ε-NH_3^+ group of Lys^{18} of hCT should undergo carbamylation. From HOHAHA and ROESY spectra of heat treated hCT, sequential NOEs ($d_{\alpha N}$ and d_{NN}) between Cys^1 and Gly^2 were observed, as well as a cross peak between the carbamyl NH_2 group and NH of Cys^1 (Figure 1-14b). However, new peaks of ε-CH_2 belonging to Lys^{18} were not detected, which would suggest that the ε-amino group of Lys^{18} is not carbamylated. In short, the above findings clearly indicate that only the N-terminal α-amino group of hCT becomes carbamylated in heated urea solution. All the resonance of carbamylated hCT were assigned and summarized in Table 1-3.

Time-course of ^1H NMR spectra of carbamylated hCT in urea solution. Carbamylated hCT molecules also possess the ability to fibrillate readily, even in urea solution. Time-course of the 1D and 2D HOHAHA spectra of the carbamylated hCT in urea solution showed similar features to those in aqueous solution, i.e., peaks in the N-terminal and central regions disappeared more rapidly than those in the C-terminal region (Figure 1-15). It is also interesting to note that the large shifts in the NH and Cα protons, of all residues in the N-terminal region of carbamylated hCT, from those of hCT (Figure 1-16) suggest a change in the binding affinity of urea molecules to the peptide, as well as an alteration of the peptide conformation in the N-terminal region.

Table 1-3: ^{1}H assignment and chemical shift data for carbamylated hCT (20 mg/ml) in 6 M urea solution, pH 2.9, 300 K

residue		NH	Hα	Hβ	others
1	Cys	6.86	4.52	3.11, 3.15	
2	Gly	8.58	3.88, 3.99		
3	Asn	8.39	4.74	2.82, 2.91	δNH2 6.96, 7.63
4	Leu	8.13	4.38	1.79	γC H 1.66,
					δCH3 0.89, 0.93
5	Ser	8.44	4.36	3.95	
6	Thr	7.74	4.39	4.29	γCH3 1.18
7	Cys	8.23	4.70	3.09, 3.20	
8	Met	8.49	4.54	2.01, 2.10	γCH2 2.51, 2.58
					εCH3 2.06
9	Leu	8.21	4.37	1.60	γC H 1.67,
					δCH3 0.88, 0.93
10	Gly	8.38	3.99		
11	Thr	7.97	4.30	4.13	γCH3 1.11
12	Tyr	8.26	4.66	2.97, 3.08	2,6H 7.10, 3,5H 6.80
13	Thr	8.05	4.27	4.16	γCH3 1.14
14	Gln	8.28	4.26	1.90, 1.97	γCH2 2.28
					εNH2 6.87, 7.42
15	Asp	8.38	4.68	2.73, 2.82	
16	Phe	8.18	4.55	3.01, 3.12	2,6H 7.21, 3,5H 7.30
					4H 7.27
17	Asn	8.33	4.64	2.68, 2.75	δNH2 6.93, 7.57
18	Lys	7.97	4.10	1.55	γCH2 1.38, δCH2 1.08
					εCH2 3.00
19	Phe	8.07	4.58	2.93, 3.11	2,6H 7.23, 3,5H 7.32
					4H 7.27
20	His	8.32	4.67	3.05, 3.16	2H 8.54, 4H 7.09
21	Thr	8.09	4.29	4.10	γCH3 1.12
22	Phe	8.38	4.90	2.92, 3.17	2,6H 7.30, 3,5H 7.33
					4H 7.30
23	Pro		4.46	1.93, 2.28	γCH2 1.99
					δCH2 3.59, 3.80
24	Gln	8.54	4.40	2.00, 2.11	γCH2 2.40
					εNH2 6.84, 7.55
25	Thr	8.15	4.34	4.22	γCH3 1.21
26	Ala	8.33	4.40	1.37	
27	Ile	8.12	4.16	1.84	γCH2 1.19, 1.49
					γCH3 0.91, δCH3 0.86
28	Gly	8.43	3.98		
29	Val	7.97	4.15	2.09	γCH3 0.92, 1.00
30	Gly	8.44	3.94		
31	Ala	8.13	4.59	1.36	
32	Pro		4.38	1.93, 2.29	γCH2 2.01
					δCH2 3.66, 3.78
					NH2 6.98, 7.61

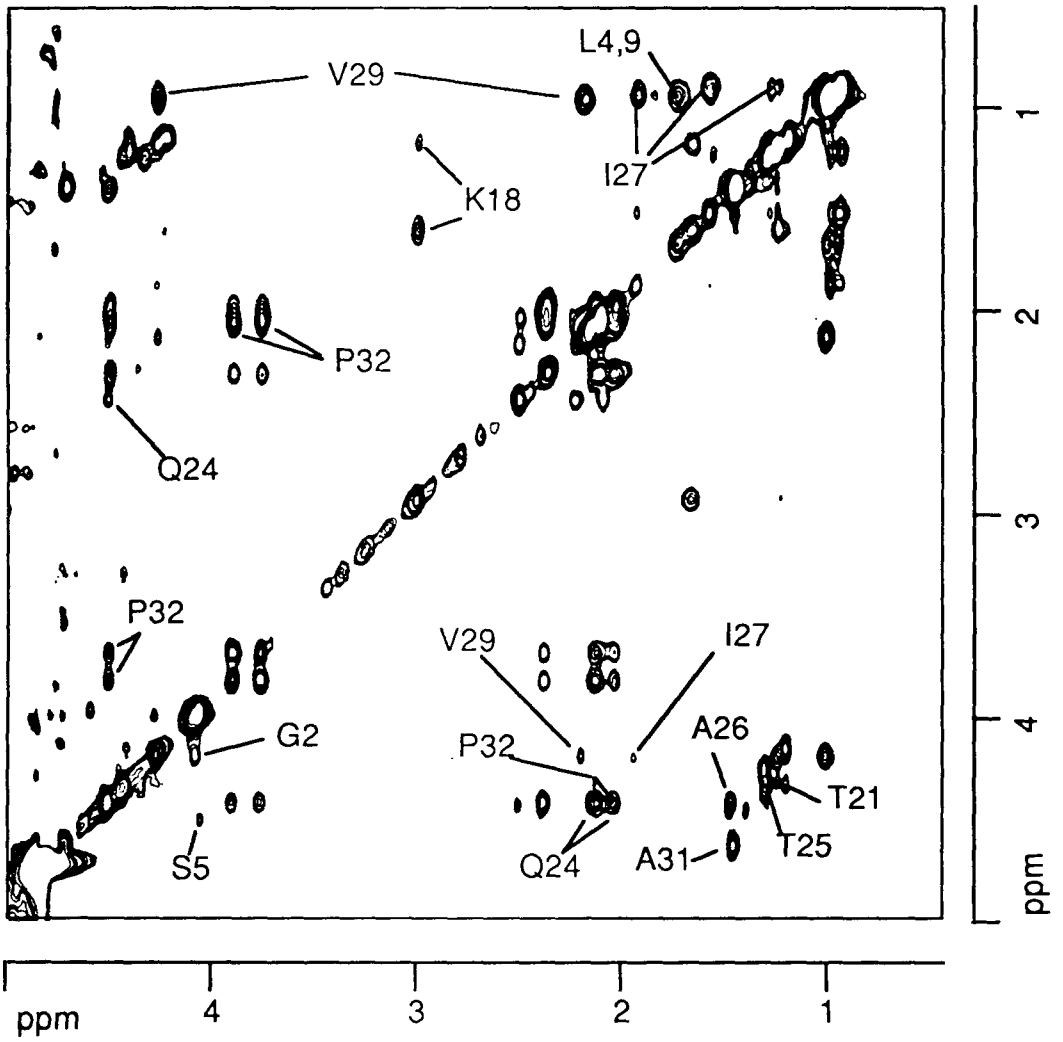

Figure 1-15: HOHAHA (80 ms) spectra of carbamylated hCT in 6 M urea solution 1 h after hCT is carbamylated. Cross peaks are labeled with their amino acid residue name (single letter code) and sequence number.

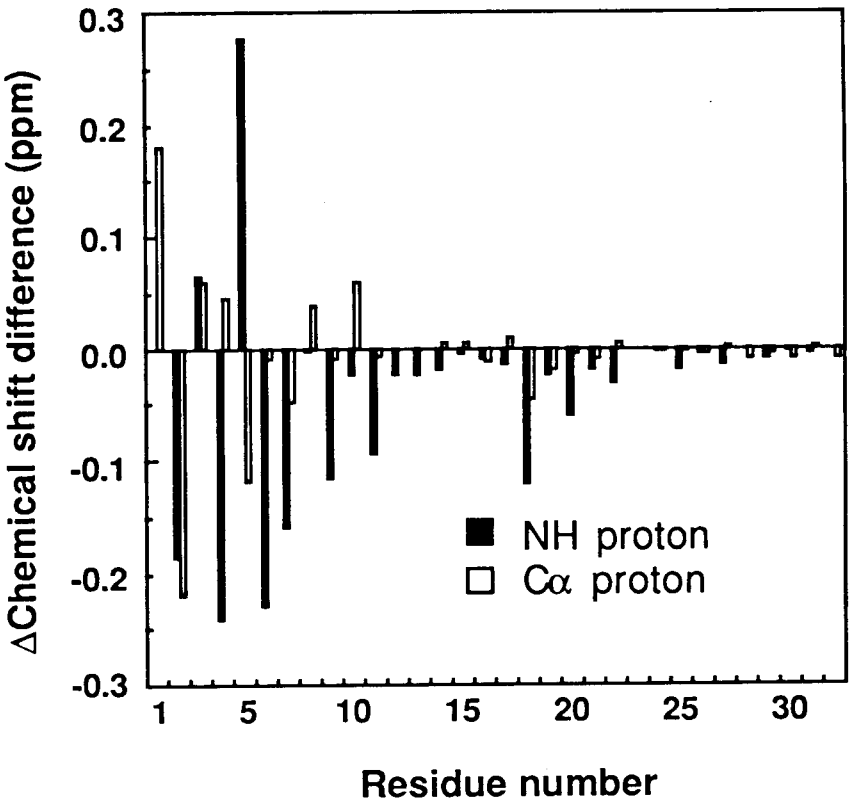

Figure 1-16: Differences in the chemical shifts of the NH (solid bars) and Cα (open bars) protons of carbamylated hCT, from the values of hCT in 6 M urea solution at 300 K and pH 2.9.

Discussion

The hCT fibrillation mechanism conforms to the double nucleation mechanism (Arvinte et al., 1993), which postulates that polymers form by nucleation processes and that there are two clear pathways for nucleation (Scheme 1-2). The first nucleation process takes place in the bulk solution, and is called homogeneous nucleation. The second nucleation occurs on the surface of pre-existing polymers. This second process is called heterogeneous nucleation. Aggregate formation in either case is thermodynamically unfavorable until a critical nucleus size is reached (Ferrone et al., 1980, 1985; Samuel et al., 1990).

The gradual signal broadening in the spectra for 40 min after the dissolution would arise from the thermodynamically unfavorable association of monomer molecules before the formation of the critical nucleus, and the second rapid broadening would be attributed to the further development of the critical nucleus in the homogeneous nucleation. All the spectral changes observed by NMR occur around t_f, and could not provide us with information in the further maturing processes observed by electron microscopy, such as, growth and thickening of fibrils and development of new fibrils from existing one in the heterogeneous nucleation.

The gradual broadening may be caused by slow interconversions between a mixture of conformations within the NMR time scale, as reported in β-amyloid peptides (Zagorski & Barrow, 1992). The slight difference in the chemical shifts between the fibril and monomer condition might be one proof of the interconversions between monomer and associated hCT molecules. The observed chemical shifts of the peptide peaks would reflect averaged structure of the monomer and associated hCT. The chemical shift and/or J coupling in the associated

hCT would differ from those in the monomer hCT, which causes the exchange broadening.

Thermodynamic study indicated that protein association consists of two steps, that is, the mutual penetration of hydration layers, causing disordering of the solvent, followed by further short-range interactions (Ross & Subramanian, 1981). During the hCT fibrillation, the cross peaks of Cα and exchangeable NH proton broadened and disappeared faster than those among non-exchangeable protons. The hydration layer of the associated hCT would be expected to differ from that of the monomer. The change in hydration layer of the associated hCT will be one of the reasons for the signal broadening.

Consequently, residues whose peaks broaden faster are strongly involved in the association before the gelation. However, after the gelation, the increase in viscosity is a dominant factor for the rapid broadening.

In TFE/H_2O solution, hCT consists of an α-helix in the central region (Doi et al., 1990). The α-helix is reported to be of the amphiphilic type, where all hydrophobic residues are oriented towards one side (Figure 1-17). The hydrophobic side of the helix contains Met^8, Leu^9, Tyr^{12}, Asp^{15}, and $Phe^{16,19,22}$. All these residues belong to the Group A whose ROESY cross peaks disappeared faster in the course of the fibrillation. On the other hand, the hydrophilic side contains residues belonging to the Group B whose ROESY peaks disappeared slowly (Figure 1-8). These results suggest that the residues of the Group A participate in the initial association step, and that the hydrophobic intermolecular interaction between residues of the Group A is particularly important for the association of hCT. If hCT molecules are associated by the hydrophobic interaction of the residues in the Group A, the initial cluster might be a helical bundle where the hydrophobic side of the amphiphilic helices

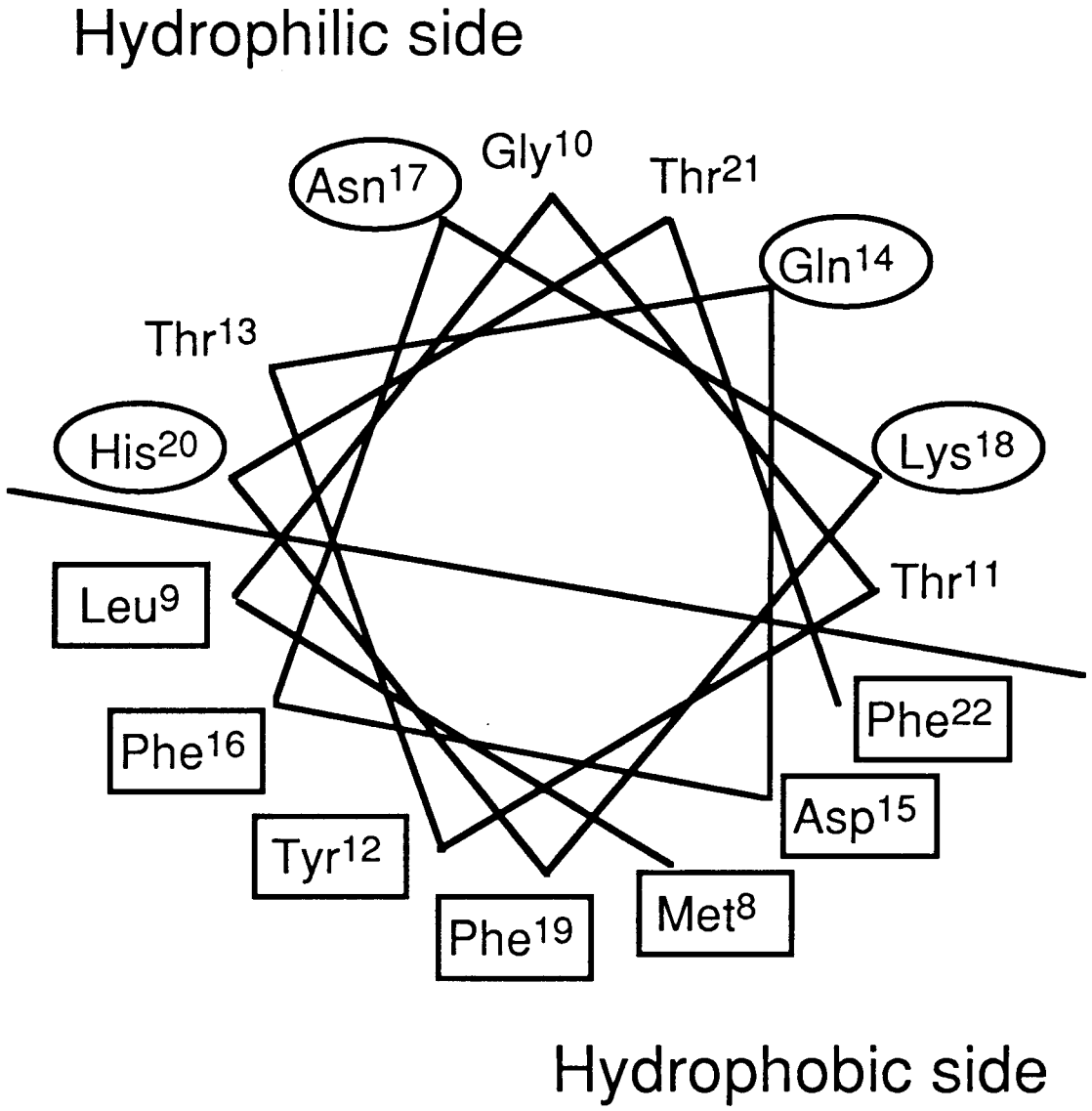

Figure 1-17: Helical wheel model of hCT in the residue range (Met^{8}-Phe^{22}). Square boxes indicate the residues whose peak belong to the Group A whereas circle boxes indicate those to the Group B.

interact with each other. This idea is in accord with the CD results of hCT fibrillation that hCT takes an α-helical structure with time (Arvinte et al., 1993). Recent study on the self-association of N-terminal fragments of barnase suggested that such an amphiphilic feature of peptide could contribute to the formation of a stable helical structure through aggregation (Yoshida et al., 1993).

The ROESY cross peaks of the N-terminal residues, Cys^1 and Leu^4, also disappeared rapidly, despite the fact that they are not included in the amphiphilic helix part. An explanation for this behavior is that Leu^4 is located at the starting point of the α-helix (Motta et al., 1991a), and that the β-protons of Cys^1, which are located near Met^8 and Leu^9, become involved in the hydrophobic cluster.

The previous results obtained by FTIR (Arvinte et al., 1993) suggested the existence of an intermolecular β-sheet in the tail region (residues 23-32) of the matured hCT fibrils 1000 min after dissolution. The broadening feature of the peaks in the C-terminal region suggests that it takes part in the fibrillation after the interaction of the N-terminal and central regions (e.g., helical bundle formation). The C-terminal region may orient the helical bundles by forming intermolecular β-sheet, leading to development of the aggregates.

As mentioned above, there is chemical exchange between the monomer and associated hCT. The slow H-D exchange rate of the N-terminal and central residues in the fibril condition indicates hydrogen bond formation in these regions of the associated hCT. The inter-molecular side-chain to backbone amide hydrogen bonding would occur during the aggregation, as reported for amyloid β-peptides (Zagorski & Barrow, 1992). It would be also possible that the formation of intra-molecular hydrogen bonds is induced by secondary structure stabilized by intermolecular interactions, such as, hydrophobic interaction.

We interpret the hCT fibrillation process in terms of the following model: In the homogeneous nucleation step, the association of hCT monomers proceeds by the intermolecular hydrophobic interaction of the residues in the N-terminal and central regions. The amphiphilicity of hCT is important for the hydrophobic interaction, and the helical bundle might be formed in the critical nucleus, which in turn induces the formation of the hydrogen bonds. The C-terminal region subsequently becomes a template for the α-helical rods in the following stage of the fibrillation (Arvinte et al., 1993).

The results of ^{1}H NMR spectra in urea solution suggests that conformational details of the amino acid side chains appear to be preserved in the presence of urea. Liepinsh & Otting (1994) defined the binding constants of urea molecules to proteins to be less than 1, by measuring the chemical shift of the protein resonance as a function of urea concentration. The similar changes of the NH chemical shifts observed in the case of hCT indicate that the binding constants of urea with hCT are small, and that urea molecules interact weakly with hCT monomer, possibly through hydrogen bonding to the amino and carbonyl groups of the peptide. It coincides with the fact that observed negative binding enthalpies for urea-protein interactions, suggesting the existence of hydrogen bonding between urea and exposed polar groups on the protein (Makhatadze & Privalov, 1992), most notably with the backbone amide and carbonyl groups (Robinson & Jencks, 1965; Nozaki & Tanford, 1970).

From previous studies that have used the chemical shift of Cα protons as an indicator of secondary structure (Wishart et al., 1991), the downfield shifts of Cα protons in urea solution (Figure 1-13) usually suggest a decrease in the α–helicity of the N-terminal and central regions. Since hCT molecules are considered to exist in a rapidly

interconverting mixture of several conformers, the proposed decrease in the α-helicity indicates an increase in concentration of conformer with extended structure, for urea solutions of hCT. It is hypothesized that the fibril nucleus consists of a helical bundle held together by hydrophobic interactions in the N-terminal and central regions, and is stabilized by inter- and/or intra-molecular hydrogen bonds (Arvinte et al., 1993). It is considered that urea, a well-known denaturant for proteins, would not initiate protein unfolding by actively disrupting the native protein conformation, but would stabilize spontaneously formed, unfolded protein, because of the weak interaction of urea with proteins (Liepinsh & Otting, 1994). Since the interaction between urea and hCT is similarly weak, it would be unlikely that the fibril core disaggregates by direct interaction with urea. As above-mentioned, there is an equilibrium between associated and monomeric hCT, conforming to the double nucleation mechanism (Ferrone et at., 1980, 1985; Samuel et al., 1990). The increase of the extended conformations would be unfavorable to form the helical bundle which is required to initiate the formation of fibril nucleus. In this regard, the stabilization of the extended form of hCT molecule is considered central to the prevention of the fibrillation. Prior to formation of the critical nucleus, the association is thermodynamically unfavorable, but upon nucleus formation, the association proceeds rapidly and spontaneously. The equilibrium may be shifted to the dissociation of the aggregates to the monomers through the interaction with urea molecules, which could explain why the fibril nucleus of hCT, that remains after lyophilization of the hCT fibril, disentangles to form monomers in urea solution.

The loss of the N-terminal charge by carbamylation increases the hydrophobicity in the N-terminal region, and hence reduces the electrostatic repulsion between hCT molecules. Thus, occurrence of the

slow carbamylation at the N-terminal α-amino group explains the gradual precipitation of hCT in urea solution after several days at room temperature. In the case of the aggregation and precipitation of apomyoglobin in aqueous urea solution, the concentration of the protein decreased approximately 6% a day, and is considered to arise from the covalent modification of lysine groups (De Young et al., 1993). It was reported that hCT derivatives whose N-terminal charge has been eliminated, fibrillate at very low concentrations, as compared to hCT (Arvinte et al., 1992). The strong hydrophobic interaction in the N-terminal and central regions causes the fibrillation even in urea solution, indicating that the fibril core formed by the strong interaction is unable to disaggregate to the monomeric form. This phenomenon is considered analogous to the mechanism that a stable protein, BPTI, is unable to unfold even in highly concentrated urea solution (Kim & Woodward, 1993; Liepinsh & Otting, 1994). In another theoretical study on protein aggregation (Fields et al., 1992), hydrophobic interactions drive protein to aggregate as an entangled network of denatured chains, and the denaturant-mediated disaggregation is predicted to be very sensitive to amino acid composition.

Time-course of the 2D NMR spectra of carbamylated hCT serves to strengthen the argument that association of carbamylated hCT is initiated in the N-terminal and central regions, with the C-terminal region subsequently becoming involved in the actual fibrillation as well as that of non-carbamylated hCT. Since the hydrophobic interactions in the N-terminal and central regions contribute to initiating the association of hCT, the association of carbamylated hCT, which is more hydrophobic, would be conducted by hydrophobic interactions in these regions.

Our results demonstrate that the hCT fibrillation is sensitive to slight changes in the hydrophobicity in the N-terminal region. The fibrillation

of sCT occurs much slower than that of hCT, and sCT is highly stable in aqueous solution (Arvinte et al., 1993). The comparison of amino acid sequence of hCT and sCT shows only small differences in the respective hydrophobicity for each residue in the hydrophobic side of the amphiphilic helix of hCT(->sCT); Met^{8}(->Val), Tyr^{12}(->Leu), Asp^{15}(->Glu), Phe^{16}(->Leu), Phe^{19}(->Leu), and Phe^{22}(->Tyr). This suggests that the difference in the fibrillation features between hCT and sCT arises from the overall electrostatic and hydrophobic effects of the molecule.

Bearing in mind the comparison on salmon CT, it can be hypothesized that by decreasing the hydrophobicity in the N-terminal and central regions of hCT, the prevention of hCT fibrillation can be attained.

1.5 Conclusions

The fibrillation of hCT has been investigated by NMR in aqueous solution. The time-course of proton 1D and 2D NMR spectra of hCT (80 mg/mL at pH 2.9) was measured during the fibrillation. It showed a gradual broadening of the peptide peaks, followed by a rapid broadening and subsequent disappearance of the peaks. The gradual broadening can be attributed to equilibrium between monomer and associated hCT, whereas the rapid broadening can be attributed to formation of aggregates and to gelation of the peptide solution. All the peptide peaks did not broaden and disappear simultaneously. Peaks of residues in the N-terminal (Cys^{1}-Cys^{7}) and central (Met^{8}-Pro^{23}) regions broadened and disappeared faster during the gradual broadening than those in the C-terminal region (Gln^{24}-Pro^{32}). Moreover, in the N-terminal and central residues, peaks of Cys^{1}, $Leu^{4,9}$, Met^{8}, Tyr^{12}, Asp^{15}, and $Phe^{16,19,22}$ disappeared faster than those of $Asn^{3,17}$, Ser^{5}, Cys^{7}, Gln^{14}, Lys^{18}, and His^{20}. Hydrogen-deuterium exchange of amide protons indicated the formation of hydrogen bonds caused by association of hCT molecules. The amphiphilicity of the peptide appears to be important for the hCT association.

The inhibitory effects of urea on the normally rapid fibrillation of hCT were also investigated by ^{1}H NMR. From subtle differences in the chemical shift of hCT in the presence and absence of urea, the occurrence of weak interactions between urea and hCT were confirmed. The chemical shifts on the NH and Cα protons of residues in the C-terminal (Gln^{24}-Pro^{32}) region were unaffected by the urea interactions, whilst the chemical shifts of the N-terminal (Cys^{1}-Cys^{7}) and central (Met^{8}-Pro^{23}) residues were observed to move significantly downfield with increasing urea concentrations. These findings suggest that urea serves to stabilize

the monomeric form of hCT and to promote the concentration of the extended hCT conformer. However, it was also found that even by storing hCT in urea the fibrillation process can not be circumvented, as the gradual carbamylation of the N-terminus takes place. Time-course of 1D and 2D spectra of carbamylated hCT showed that cross peaks of residues in the N-terminal and central regions disappear faster than those in the C-terminal regions, indicating that the fibrillation of carbamylated hCT is initiated in the N-terminal and central regions. It is postulated that carbamylation increases the hydrophobicity of the N-terminal region and hence fosters fibrillation, even in urea solution.

Effects of urea on the peptide aggregation-disaggregation are somewhat similar to those of urea on protein folding-unfolding. Urea molecules interact weakly with hCT monomer, possibly through hydrogen bonding to the amino and carbonyl groups of the peptide, and serve to stabilize the extended conformations of hCT, which lead to the disentanglement of the fibril core and inhibition of fibrillation. However, the strong hydrophobic interaction in the N-terminal and central regions resulting from carbamylation of the N-terminal amino group, by decomposition of an urea molecule, significantly promotes the fibrillation in urea solution. All these results suggest that the problems of hCT fibrillation in therapeutic uses may be circumvented by the addition of compounds which form hydrogen bonds with the peptide molecule or induce a slight decrease of the hydrophobicity in the N-terminal and central regions of the peptide.

1.6 References

Arvinte, T., Cudd, A., & Drake, A. F. (1993) *J. Biol. Chem. 268*, 6415-6422.

Arvinte, T., & Ryman, K. (1992) European Patent Application, Publication Number 0490549A.

Austin, L. A., & Heath, H. (1981) *N. Engl. J. Med. 304*, 296-297.

Bax, A., & Davis, D. G. (1985) *J. Magn. Reson. 63*, 207-213.

Billeter, M., Braun, W., & Wüthrich, K. (1982) *J. Mol. Biol. 155*, 321-346.

Braunschweiler, L., & Ernst, R. R. (1983) *J. Magn. Reson. 53*, 521-528.

Copp, D. H., Cameron, E. C., Cheney, B. A., Davidson, A. G. F., & Henze, K. G. (1962) *Endocrinology 70,* 638-649.

Davis, D. G., & Bax, A. (1985) *J. Am. Chem. Soc. 107*, 2820-2821.

De Young, L. R., Dill, K. A., & Fink, K. (1993) *Biochemistry 32,* 3877-3886.

Doi, M., Yamanaka, Y., Kobayashi, Y., Kyogoku, Y., Takimoto, M., & Goda, K. (1990) *Peptides: Chemistry, Structure & Biology, 11th Proc. Am. Pept. Symp., July 9-14, 1989, Lajolla, CA.*, (Rivier, J. E. & Marshall, G. R., Eds.) p.165-167, ESCOM, Leiden, The Netherlands.

Ferrone, F. A., Hofrichter, J., Sunshine, H. R., & Eaton, W. A. (1980) *Biophys. J. 32*, 361-380.

Ferrone, F. A., Hofrichter, J., & Eaton, W. A. (1985) *J. Mol. Biol. 183*, 611-631.

Fields, G. B., Alonso, D. O. V., Stigter, D., & Dill, K. A. (1992) *J. Phys. Chem. 96,* 3974-3981.

Jarvis, A. J., Munro, S. L. A., & Craik, D. J. (1994) *Biochemistry 33,* 33-41.

Jeener, J., Meier, B. H., Bachmann, P., & Ernst, R. R. (1979) *J. Chem. Phys. 71,* 4546-4553.

Kern, D., Drakenberg, T., Wikström, M., Forsén, S., Bang, H., & Fischer, G. (1993) *FEBS Lett. 323*, 198-202.

Kim, K. -Y, & Woodward, C. (1993) *Biochemistry 32,* 9609-9613.

Kumar, M. A., Foster, G. V., & MacIntyre, I. (1963) *Lancet 2,* 480-482.

Liepinsh, E., & Otting, G. (1994) *J. Am. Chem. Soc. 116,* 9670-9674.

Lumb, K. J., & Dobson, C. M. (1992) *J. Mol. Biol. 227,* 9-14.

Macura, S., Huang, Y., Suter, D., & Ernst, R. R. (1981) *J. Magn. Reson. 43*, 259-281.

Makhatadze, G. I., & Privalov, P. L. (1992) *J. Mol. Biol. 226,* 491-505.

Marion, D., & Wüthrich, K. (1983) *Biochem. Biophys. Res. Commun. 113*, 967-974.

Marion, D., Ikura, M., Tschudin, R., & Bax, A. (1989) *J. Magn. Reson. 85*, 393-399.

Meadows, R. P., Nikonowicz, E. P., Jones, C. R., Bastian, J. W., & Gorenstein, D. G. (1991) *Biochemistry 30*, 1247-1254.

Meyer, J. P., Pelton, J. T., Hoflack, J., & Saudek, V. (1991) *Biopolymers 31*, 233-241.

Motta, A., Pastore, A., Goud, N. A., & Morelli, M. A. C. (1991a) *Biochemistry 30*, 10444-10450.

Motta, A., Temussi, P. A., Wünsch, E., & Bovermann, G. (1991b) *Biochemistry 30*, 2364-2371.

Nozaki, J., & Tanford, C. (1970) *J. Biol. Chem. 245,* 1648-1652.

Piantini, U., Sørensen, O. W., & Ernst, R. R. (1982) *J. Am. Chem. Soc. 104*, 6800-6801.

Pike, A. C. W., & Acharya, K. R. (1994) *Protein Sci., 3,* 706-710.

Rance, M., Sørensen, O. W., Bodenhausen, G., Wagner, G., Ernst, R. R., & Wüthrich, K. (1983) *Biochem. Biophys. Res. Commun. 117*, 479-485.

Robinson, D. R., & Jencks, W. P. (1965) *J. Am. Chem. Soc. 87,* 2462-2470.

Ross, P. D., & Subramanian, S. (1981) *Biochemistry 20,* 3096-3102.

Samuel, R. E., Salmon, E. D., & Briehl, R. W. (1990) *Nature 345*, 833-835.

Sieber, P., Riniker, B., Brugger, M., Kamber, B., & Rittel, W. (1970) *Helv. Chim. Acta 53*, 2135-2150.

Stark, G. R., Stein, W. H., & Moore, S. (1960) *J. Biol. Chem. 235,* 3177-3181.

Wishart, D. S., Sykes, B. D., & Richards, F. M. (1991) *J. Mol. Biol. 222,* 311-333.

Wüthrich, K., Wider, G., Wagner, G., & Braun, W. (1982) *J. Mol. Biol. 155*, 311-319.

Yoshida, K., Shibata, T., Masai, J., Sato, K., Noguti, T., Go, M., & Yanagawa, H. (1993) *Biochemistry 32*, 2162-2166.

Zagorski, M. G., & Barrow, C. J. (1992) *Biochemistry 31*, 5621-5631.

Chapter 2

^{113}Cd NMR Studies of Cabbage Histidinol Dehydrogenase

Abbreviations

HDH, histidinol dehydrogenase; [Zn]HDH, wild type HDH containing Zn ; [^{113}Cd]HDH, ^{113}Cd-substituted histidinol dehydrogenase; Tris, tris(hydroxy-methyl)aminomethane; EDTA, ethylenediaminetetraacetic acid; LADH, horse liver alcohol dehydrogenase; T_1, spin-lattice relaxation time; HMQC, heteronuclear multiple quantum coherence

2.1 Introduction

Histidinol dehydrogenase (HDH) [L-histidinol:NAD oxidoreductase (EC 1.1.1.23)] is an NAD^+-dependent enzyme that catalyzes the two final reaction steps in histidine biosynthesis, from L-histidinol over L-histidinal to L-histidine (Scheme 2-1) (Adams, 1955). The understanding of the function-structure relationship of HDH will be used for the rational design of enzyme inhibitors, leading to the discovery of unknown herbicidal lead structures and principles.

Scheme 2-1: HDH catalytic reaction

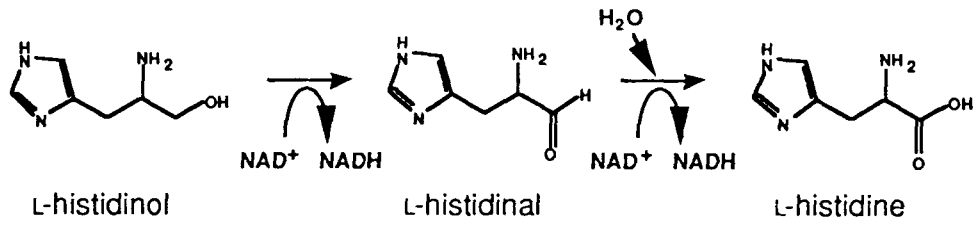

The active enzyme is a homodimer with a molecular weight of about 100,000. Each subunit contains one Zn(II) ion. The removal of the metal ion from HDH abolishes the enzymatic activity (Lee & Grubmeyer, 1987). To date, limited information about the state of the metal ion is available. It is even unknown whether the metal ion is actually involved in the catalytic reaction of HDH or not. Recently, site-specific mutagenesis has been developed for studying the role of conserved cysteine residues in HDH from *Salmonella typhimurium* (Teng et al., 1993) and *Cabbage* (Nagai et al., 1993). Both studies indicate that the conserved cysteine residues in HDH are not liganded to the metal ion, and that HDH does not use a cysteine-based thiohemiacetal as a catalytic intermediate. X-ray crystallographic study on HDH has not been reported yet.

Cd(II) can often be substituted for Zn(II) at the active site of the metalloenzymes with retention of activity (Chlebowski & Coleman, 1976; Omburo et al., 1993). Hence metal ions in several zinc metalloenzymes have been explored by ^{113}Cd NMR spectroscopy (Summers, 1988). The chemical shift and line width of ^{113}Cd are sensitive to the number, type, geometry, and dissociation constant of its ligands. For proteins whose X-ray structural data are not available, ^{113}Cd NMR is used to provide a first-approximation of the ligands at the metal binding sites. In many cases, ^{113}Cd NMR spectroscopy has provided new insights into protein-substrate interactions, conformational changes, and metal displacement reactions.

In this study, HDH apoenzyme (Nagai et al., 1992; Nagai & Ohta, 1994) was reconstituted by adding 1 mol of cadmium per mol of subunit. The ^{113}Cd-substituted HDH ([^{113}Cd]HDH) exhibited the same catalytic activity as [Zn]HDH. In order to elucidate the role of the metal ion and the reaction mechanism of HDH, ^{113}Cd NMR spectra of [^{113}Cd]HDH have been recorded in the complexes with the two substrates and four inhibitors (imidazole, histamine, L-histidine, and DL-4-(4-imidazolyl)-3-amino-2-butanone) in the absence and presence of NAD^+.

The enhancement of HDH catalytic reaction will also be discussed. We found that Cd^{2+} enhanced the activity by maximally 75% like Mn^{2+}. It was previously reported that additional Mn^{2+} in the reaction mixture stimulates the HDH reaction (Loper & Adams, 1965), whereas all other divalent cations such as Zn^{2+}, Mg^{2+}, Ni^{2+}, Co^{2+}, Cu^{2+}, and so on depressed it (Nagai & Scheidegger, 1991; Grubmeyer et al., 1989). Although Zn^{2+} ion of [Zn]HDH is known to be replaced by the added Mn^{2+} under alkaline conditions (Grubmeyer et al., 1989), the stimulatory mechanism of Mn^{2+} has not been elucidated. ^{113}Cd NMR is, in particular, useful for studying the kinetics of metal displacement

reactions (Otvos et al., 1980; Sudmeier et al., 1980; Pan et al., 1993; Omburo et al., 1990). Effects of the additional metal ion on the structural change around the metal binding site were investigated by ^{113}Cd NMR spectroscopy.

2.1 Materials and methods

Materials. ^{113}Cd metal (95 atom %) was obtained from ISOTEC Inc. (Miamisburg, Ohio). $[^{113}Cd]SO_4$ was prepared by a following procedure. 46.5 mg of ^{113}Cd metal was dissolved in 80 μL concentrated nitrate acid. After the metal was completely dissolved, 2 M ammonium carbonate was added and then precipitate of cadmium carbonate was filtered off, washed by water, and dried. Diluted sulfuric acid was added to the powder of cadmium carbonate until the evolution of carbon dioxide stopped. The solution of cadmium sulfate was stored at the concentration of 100 mM. Nonlabeled $CdSO_4$ was purchased from Nacalai Tesque (Kyoto, Japan).

NAD^+ and L-histidinol were purchased from Sigma (St. Louis, MO). Imidazole was obtained from Wako Pure Chemical Industries, Ltd. (Osaka), and L-histidine and histamine derived from Tokyo Kasei Kogyo Co., Ltd. (Tokyo). DL-histidinal and DL-4-(4-imidazolyl)-3-amino-2-butanone were prepared by the following manner. To a suspension of DL-histidine in MeOH, $SOCl_2$ was added at -20 °C and the mixture was stirred for 18 h at room temperature to give DL-histidine methylester HCl. Then, the methyl ester was treated with BOC anhydride in Acetone-H_2O (1:1) in the presence of Et_3N to give N_α, N_{im}-di-BOC-DL-histidine methylester. The protected methylester was reduced with diisobutylaluminium hydride in THF to give N-BOC-2-amino-3-(1-BOC-imidazol-4-yl)-propanol, followed by oxidation reaction with activated dimethylsulfoxide in CH_2Cl_2 to afford N-BOC-2-amino-3-(1-BOC-imidazol-4-yl)-propionaldehyde (di-BOC-DL-histidinal) (Mancuso et al., 1978). The aldehyde was deprotected with 4N-HCl in dioxane (or 30% HBr in CH_3COOH) to give DL-histidinal [2-amino-3-(1H-imidazol-4-yl)-propionaldehyde] HCl (or HBr) salt. The reaction of di-BOC-DL-histidinal with methylmagnesium chloride in THF gave N-BOC-2-amino-

3-(1-BOC-imidazol-4-yl)-1-methyl-propanol, followed by oxidation reaction using periodinane (Dess & Martin, 1983) to afford N-BOC-3-amino-4-(1-BOC-imidazol-4-yl)-2-butanone. The deprotection reaction was performed in the same manner with di-BOC-DL-histidinal to give DL-4-(4-imidazolyl)-3-amino-2-butanone HCl (or HBr) salt (Smissman & Weis, 1971). All compounds exhibited ^{1}H NMR and infrared spectra in agreement with assigned structure.

Enzyme preparation. HDH used in this study was purified from a nuclear polyhedrosis virus genome expression system containing the plasmid pVL1393 (Summers & Smith, 1987; Nagai et al., 1992). The purification protocol of HDH is the same as that previously described in the Appendix 2.1 (Nagai et al., 1991, 1993). Typically, infected insect cells (ca. 600 mg cellular protein) were harvested from 1 L of culture medium by centrifugation at 3,500 X g for 10 min and then homogenized, in 50 mL 20 mM Tris-HCl (pH 7.4) containing 100 μM EDTA, 1 μM leupeptin, 1 μM pepstatin A, and 200 μM PMSF, by sonic treatment for 30 s for three times at a medium intensity setting in a Branson sonicator (Sonifier 450). After centrifugation at 10,000 X g for 15 min, the supernatant was subjected to two-step anion exchange chromatography on first a DEAE-Toyopearl (5 X 6 cm) column and then second a Mono Q (HR 16/10) column in a FPLC system (Pharmacia). The purified proteins were analyzed by sodium dodecyl sulfate polyacrylamide gel electrophoresis (SDS-PAGE), using 10-20% polyacrylamide gels, according to the method of Laemmli (1970).

Preparation and reconstitution of apoenzyme. The apoenzyme of HDH was prepared as previously described (Nagai & Ohta, 1994). Solution of HDH (8 mg/mL) was incubated in 200 mM Gly-NaOH buffer (pH 9.2) containing 20 mM ethylenediaminetetraacetic acid (EDTA) at 30 °C for 1 h, followed by a Pharmacia gelfiltration NAP-10 column (Pharmacia

LKB), equilibrated in 20 mM tris(hydroxymethyl)aminomethane (Tris) -SO_4 buffer (pH 7.2). The residual metal-EDTA complex and EDTA were removed by diafiltration with an Amicon ultrafiltration device Centriprep-10 (Amicon Inc., MA) against the Tris-SO_4 buffer solution. It was confirmed that the enzymatic activity dropped to less than 1% of the initial value. As reported in the previous paper (Nagai & Ohta, 1994), Zn analysis by inductivity coupled radiofrequency plasma atomic emission spectrometry showed that the apo-HDH did not contain any detectable amounts of Zn^{2+} ion. Reconstitution of the apoenzyme was achieved by adding a [^{113}Cd]SO_4 solution to the apo-HDH solution with monitoring the enzymatic activity. About ~10% molar excess [^{113}Cd]SO_4 to the subunit concentration of the apoenzyme was added, followed by dialysis against the Tris-SO_4 buffer in order to remove the excess metal salt. The enzymatic activity of reconstituted [^{113}Cd]HDH was not decreased by dialysis at all.

Enzyme assays. The enzyme concentration was determined spectroscopically by using an $A^{1\%}$ at 280 nm = 7.98. The enzymatic activity was routinely determined by monitoring the change in absorbance at 340 nm due to the conversion of NAD^+ to NADH. The reaction mixture contained 25 mM Bis-Tris-propane (pH 7.2), 0.5 mM NAD^+, 0.25 mM L-histidinol, and 1-2 mU of enzyme sample in a total volume of 2.0 mL. The reaction was performed at 30 °C, and started by addition of L-histidinol. We used a Hitachi U-3120 spectrophotometer.

NMR spectroscopy. ^{113}Cd NMR measurements were mainly performed on a Bruker AMX600 spectrometer (133.1 MHz for ^{113}Cd) with a 10-mm tunable broad-band probe. Spin-lattice relaxation times (T_1) were estimated by using an inversion recovery method. In order to study the ^{113}Cd relaxation mechanism, several experiments were performed on a Bruker ARX400 spectrometer (88.8 MHz for ^{113}Cd). Chemical shifts

were referred to the resonance position of 0.1 M $Cd(ClO_4)_2$. Typical acquisition parameters for AMX600 were 36000 Hz sweep width, and 16 μs pulse width (60 degree pulse) without proton decoupling. Samples were 1.8-2.0 mL (10% D_2O) of about 0.5 mM (dimer concentration) [^{113}Cd]HDH in the Tris-SO_4 solution in order to avoid the influence of halide ions on the ^{113}Cd chemical shift (Summers, 1988).

2.3 Results

2.3.1 Characterization of [^{113}Cd]HDH

Reconstitution of apo-HDH and activity of [^{113}Cd]HDH. The apoenzyme whose activity was less than 1% of that of [Zn]HDH, was reactivated with increasing amounts of [^{113}Cd]SO_4. The titration demonstrates that the activity increases linearly until the cadmium concentration is equal to the subunit concentration. The activity of [^{113}Cd]HDH, reconstituted by 1 mol of ^{113}Cd(II) per mol of subunit, was 0.77 units/mg at pH 7.2 which was equal to that of [Zn]HDH.

^{113}Cd NMR of [^{113}Cd]HDH. A titration of solutions of apo-HDH with $^{113}Cd^{2+}$ ions was performed with monitoring ^{113}Cd spectra. Figure 2-1 shows ^{113}Cd NMR spectrum of 1:1 [^{113}Cd]HDH measured at 20 °C, pH 7.2. A single resonance was observed at 110 ppm. The line widths of [^{113}Cd]HDH were about 400 Hz at 133.1 MHz and 280 Hz at 88.8 MHz. [^{113}Cd]HDH reactivated with 0.3 equiv of $^{113}Cd^{2+}$ per subunit of apo-HDH showed an resonance at 110 ppm. Its line width was equal to that of [^{113}Cd]HDH reconstituted with 1 equiv of $^{113}Cd^{2+}$ per subunit in Figure 2-1, and the intensity and catalytic activity were about 30%. This result indicates that the first two Cd^{2+} ions added to the apoenzyme dimer are bound to identical sites.

Within the temperature range from 4 to 20 °C, the chemical shift and line width of the [^{113}Cd]HDH resonance were identical while the intensity slightly increased with an increase in temperature. This indicates that the resonance is not perturbed by the chemical exchange between the bound and free states of the metal ion. The T_1 value at 133.1 MHz was estimated to be 3.5 ± 0.7 s. The line width decreased slightly, only about by 20 Hz under broad band proton decoupling.

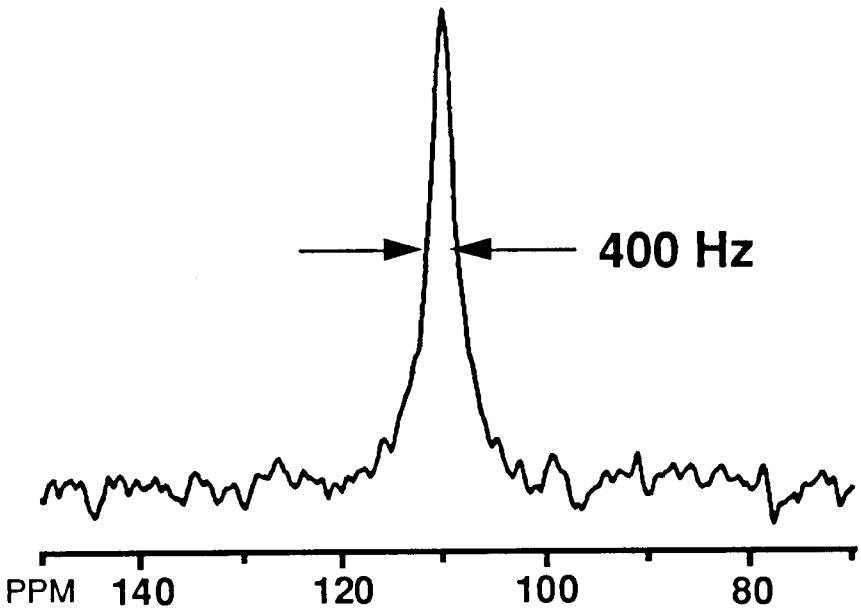

Figure 2-1: ^{113}Cd NMR spectrum of [^{113}Cd]HDH in 20 mM Tris-SO_4, 20 °C. The number of scans is 30,000, and the relaxation delay was 4 s. A 100 Hz line broadening was applied.

The effect of pH on the chemical shift and line width of [^{113}Cd]HDH was examined. In the pH range 6-7.5, no significant change was observed in the ^{113}Cd spectra, but in the pH range 8-9 where the enzyme shows the highest activity (pH 9.2), the ^{113}Cd resonance broadened and disappeared (Figure 2-2), and a slight downfield shift (< 1 ppm) was observed with an increase of pH.

^{113}Cd NMR signal generally exhibits downfield shifts with an increase of chloride ion concentration if the external medium is accessible to the metal ion, (Summers, 1988). The chemical shift and line width of [^{113}Cd]HDH were unaffected by the presence of chloride ion (0-300 mM) at pH 7.2, indicating that the metal binding site of HDH is not solvent accessible.

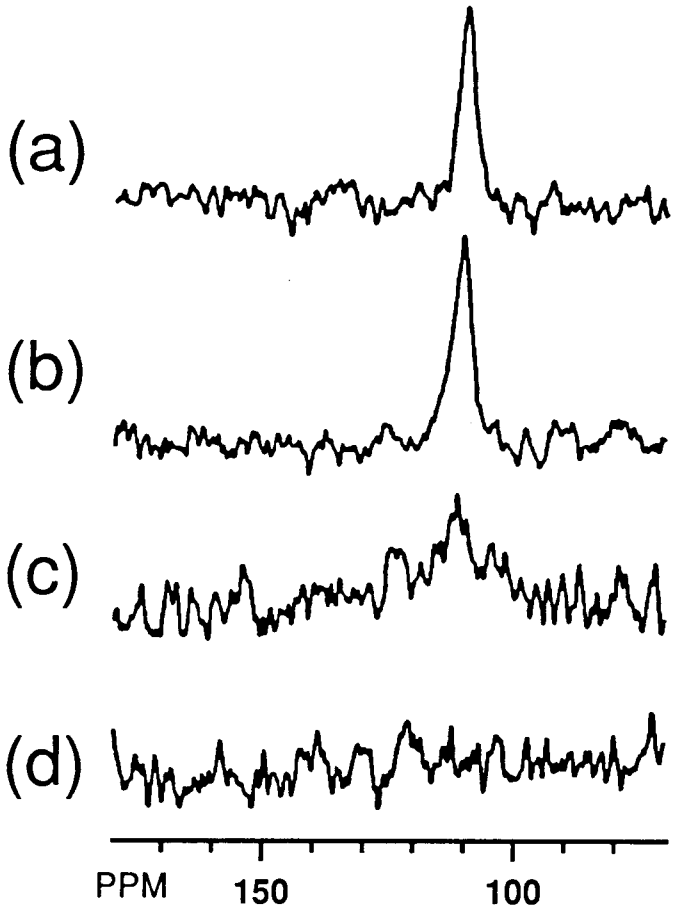

Figure 2-2: ^{113}Cd NMR spectra of [^{113}Cd]HDH at various pH values. The number of scans is given in the parentheses. The relaxation delays were 4 s for all spectra. A 100 Hz line broadening was applied. (a) pH 6.2 (15,000). (b) pH 7.2 (15,000). (c) pH 8.3 (90,000). (d) pH 8.8 (20,000).

2.3.2 Effect of excess Cd^{2+} ion on the catalytic activity

Catalytic activity of [Zn]HDH in the presence of excess Cd^{2+}. The enhancement of the catalytic activity of [Zn]HDH with increasing amounts of $CdSO_4$ is shown in Figure 2-3. The titration demonstrated that the stimulatory effect of Cd^{2+} was saturated between 20-200 μM $CdSO_4$, and slowly decreased with a further increase of the Cd^{2+} concentration ($[Cd^{2+}] > 200$ μM). The HDH reaction was stimulated about maximally 75% by the addition of Cd^{2+}. The catalytic activity of [^{113}Cd]HDH in the titration of Cd^{2+} showed the same feature as that of [Zn]HDH.

^{113}Cd NMR spectra of [Zn]HDH in the presence of $^{113}Cd^{2+}$. [Zn]HDH in the presence of $^{113}Cd^{2+}$ ion showed no peaks (data not shown), and even a peak from free $^{113}Cd^{2+}$ was not detected either. The addition of excess EDTA (5-fold concentration of the protein) to the solution of [Zn]HDH at pH 7.2 and 20 °C in the presence of $^{113}Cd^{2+}$ exhibited an EDTA-bound $^{113}Cd^{2+}$ peak at 82 ppm (data not shown). This fact suggests that added $^{113}Cd^{2+}$ ions interact with some parts of the protein. One possible explanation for the inability to observe ^{113}Cd signals is chemical exchange broadening, which has been reported for ^{113}Cd NMR study of proteins (Otvos et al., 1980; Sudmeier et al., 1980; Gettins, 1980). The activity of the NMR sample after the addition of EDTA was completely retained, indicating that Zn^{2+} exists in the original site and is not removed by EDTA under these conditions. Zn^{2+} in [Zn]HDH was not replaced by the added $^{113}Cd^{2+}$, which coincides with the results that Mn^{2+} in the reaction mixture does not exchange with Zn^{2+} in HDH at pH 8 (Grubmeyer et al., 1989). It indicates that the affinity of Cd^{2+} for the original site is weaker than that of Zn^{2+}.

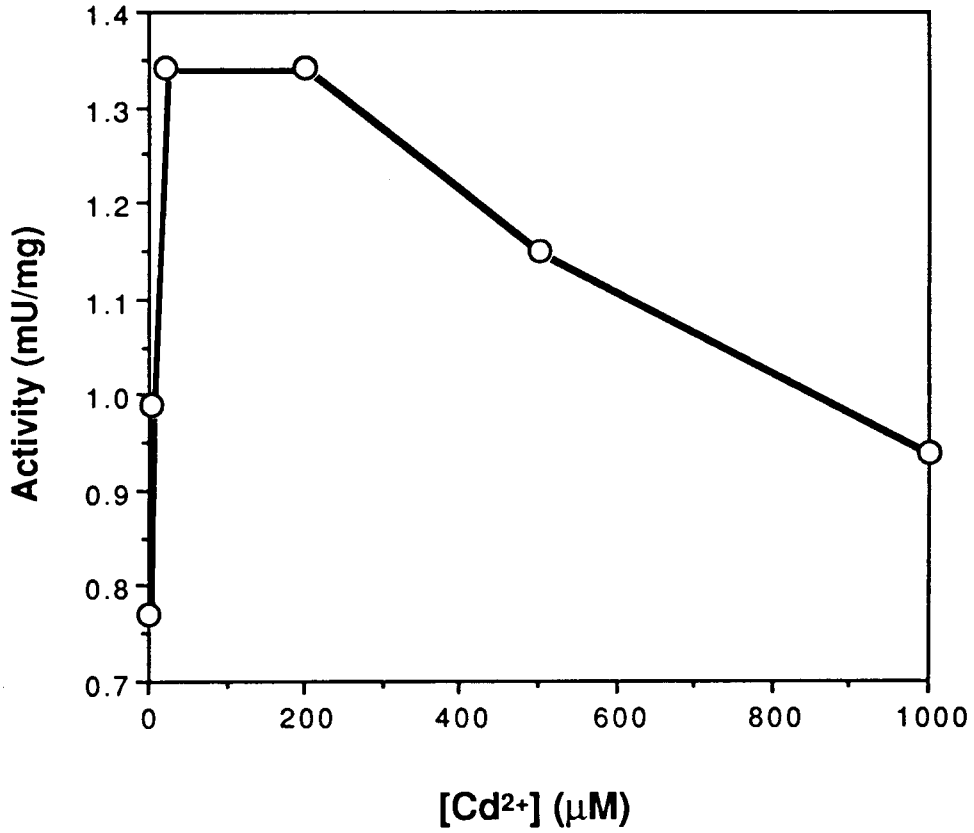

Figure 2-3: Enhancement of activity for rHDH with varying amounts of $CdSO_4$ in a reaction mixture. The reaction mixture contained 25 mM Bis-Tris-propane (pH 7.2), 0.5 mM NAD^+, 0.25 mM histidinol, and 1~2 mU of enzyme sample in a total volume of 2.0 ml. The reaction was started with the addition of histidinol, and icubated at 30 °C.

^{113}Cd NMR spectra of [^{113}Cd]HDH in the presence of $^{113}Cd^{2+}$ or nonlabeled Cd^{2+}. In the concentration range of $^{113}Cd^{2+}$ ions less than 1 equiv per subunit, only the peak at 110 ppm was observed (Figure 2-4a). The addition of $^{113}Cd^{2+}$ beyond one equiv per subunit resulted in a decrease of the signal at 110 ppm, together with a small broadening by 30 Hz, and in appearance of three additional peaks at 83, 22, and -2 ppm (Figure 2-4b). The intensity of the peak at 110 ppm in Figure 2-4b became about 70% of that in Figure 2-4a. The intensities of the two peaks at 83 and 22 ppm did not depend on the concentration of the added $^{113}Cd^{2+}$ ion while that of the peak at -2 ppm increased gradually with increasing the concentration of $^{113}Cd^{2+}$. After dialysis these three peaks disappeared (data not shown). This result indicates that Cd(II) ions predominantly bind to the major site (110 ppm) when Cd(II) ions molar equivalent to the subunit concentration were added.

As above-mentioned, on adding excess $^{113}Cd^{2+}$ ion to [^{113}Cd]HDH solution, three other peaks with weak intensities were observed at -2, 22, and 83 ppm besides the peak at 110 ppm. In order to monitor the kinetics of the displacement of $^{113}Cd^{2+}$ at the first binding site and appearance of the additional three peaks, an excess amount of nonlabeled Cd^{2+} was added to freshly prepared [^{113}Cd]HDH. Figure 2-4c and d show time dependence of ^{113}Cd spectra of [^{113}Cd]HDH in the presence of nonlabeled Cd^{2+}. First, the peaks at 110 and -2 ppm disappeared, and the other two peaks at 83 and 22 ppm remained (Figure 2-4c) where the intensities were almost similar to those in Figure 2-4b. This indicates that $^{113}Cd^{2+}$ ions represented by 83 and 22 ppm are originated from the $^{113}Cd^{2+}$ ions in the first binding site (110 ppm in Figure 2-4a). Thus, the decrease of the peak intensity at 110 ppm by the addition of excess $^{113}Cd^{2+}$ ions (Figure 2-4b) would be attributed to the increase of those at 83 and 22 ppm. The peak at -2 ppm in Fig 2b may be originated from the

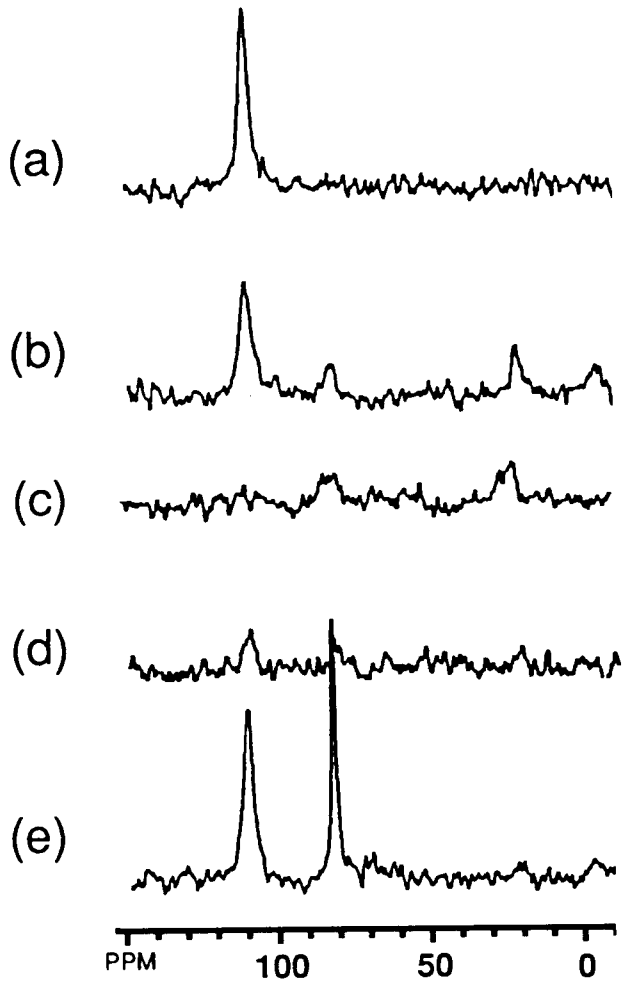

Figure 2-4: (a) The ^{113}Cd NMR spectrum of [^{113}Cd]HDH (protein dimer concentration 0.5 mM, temperature 20 °C, pH 7.2).
(b) The ^{113}Cd NMR spectrum of [^{113}Cd]HDH in the presence of 2 mM $^{113}Cd^{2+}$.
(c) The ^{113}Cd NMR spectrum of [^{113}Cd]HDH in the presence of 2 mM nonlabeled Cd^{2+}.
(d) The ^{113}Cd NMR spectrum 1 day after (c).
(e) (b) plus 2 mM EDTA. To enable intensity comparisons to be made within this series, all spectra were acquired under identical conditions as described in the text.

added $^{113}Cd^{2+}$ ions because the intensity showed the concentration dependence of $^{113}Cd^{2+}$. Hereafter, the metal binding sites represented by the peaks at 110, 83, and 22 ppm are called as A, A', and A" sites, respectively, and that at -2 ppm, as B site. Then, the ^{113}Cd NMR spectrum 1 day after Figure 2-4c exhibited that the peak at 110 ppm appeared again, and the peaks at 83 and 22 ppm became smaller (Figure 2-4d). The spectra were unchanged from Figure 2-4d, indicating that the equilibrium between A, A', A", B site Cd^{2+}, and free Cd^{2+} ions was reached. The exchange rate of A site Cd^{2+} ion with free Cd^{2+} ion is faster than that of A' and A" site Cd^{2+}. Since in the absence of excess $^{113}Cd^{2+}$ ion, extensive dialysis by Tris-SO_4 buffer can not remove $^{113}Cd^{2+}$ ion from [^{113}Cd]HDH at all, the environment around A site Cd^{2+} (the peak at 110 ppm in Figure 2-4b) may be affected by the added $^{113}Cd^{2+}$, resulting in the high dissociation constant.

^{113}Cd NMR spectra of [^{113}Cd]HDH in the titration of ethylenediaminetetraacetic acid (EDTA). In order to obtain information concerning the relative affinities of Cd^{2+} for A, A', A", and B sites, the titration of EDTA was performed for the solution of [^{113}Cd]HDH containing $^{113}Cd^{2+}$. With an increase of EDTA concentration, peaks of A', A", and B sites became smaller, and a new sharp peak at 82 ppm, which was assigned to be a signal of EDTA-bound $^{113}Cd^{2+}$, became larger (Figure 2-4e). The intensity and line width of the peak at 110 ppm in Figure 2-4e were restored as those in Figure 2-4a. The peak at 110 ppm disappeared on further addition of EDTA in large excess (5-fold concentration of the protein), and only EDTA-bound ^{113}Cd signal was observed at 82 ppm (data not shown). The catalytic activity of the NMR sample was completely lost, and all the enzyme adopts apo-form. It indicates that even Cd^{2+} at the catalytic site is removed by EDTA unlike [Zn]HDH.

2.3.3 Interaction of the catalytic metal ion with ligands

^{113}Cd NMR of binary [^{113}Cd]HDH-substrate complexes. The product inhibition patterns of HDH conformed to a Bi Uni Uni Bi Ping Pong mechanism (Bürger & Görisch, 1981; Grubmeyer et al., 1987; Kheirolomoom et al., 1994). The reaction scheme is ordered with the binding of L-histidinol first and NAD^+ second, and L-histidine as the last product to be released. *K*m values for L-histidinol and L-histidinal were, reported for [Zn]HDH, 10 and 2.7 μM, respectively (Grubmeyer et al., 1987; Nagai et al., 1992; Nagai & Ohta, 1994).

Figure 2-5a and b show the ^{113}Cd NMR spectra obtained upon titration of L-histidinol into [^{113}Cd]HDH. As the resonance of [^{113}Cd]HDH at 110 ppm became small with an increase of the L-histidinol concentration, a new resonance of the [^{113}Cd]HDH-histidinol complex appeared at 210 ppm. This shift did not depend on the concentration of L-histidinol (0.25-5 times concentration of the subunit). The peak intensity of the [^{113}Cd]HDH-histidinol complex slightly increased with an increase of temperature like that of [^{113}Cd]HDH. On the other hand, the [^{113}Cd]HDH-histidinal complex showed a signal at 192 ppm whose line width is 480 Hz at 133.1 MHz (Figure 2-5c). The line widths of the [^{113}Cd]HDH and the two [^{113}Cd]HDH-substrate complexes were measured at 133.1 and 88.8 MHz, and are summarized in Table 2-1.

The line widths of the complexes became significantly broader than that of [^{113}Cd]HDH in the absence of the ligand. Taking account of the temperature dependence of ^{113}Cd NMR spectra of the complexes, this line broadening would be attributed to the conformational change of the active site of the enzyme by the binding of the substrates but not to the

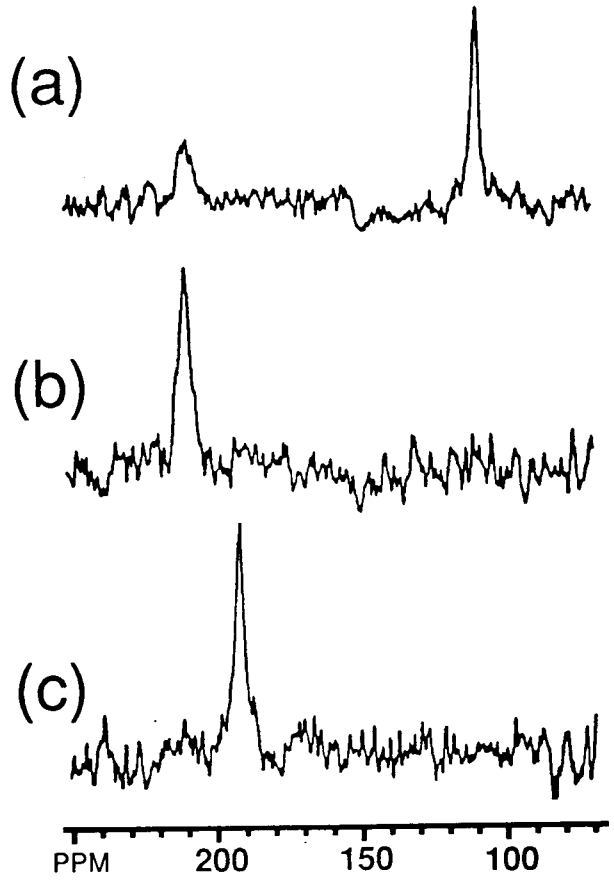

Figure 2-5: ^{113}Cd NMR spectra of the [^{113}Cd]HDH-substrate complexes in 20 mM Tris-SO_4, 20 °C. The number of scans is given in the parentheses. The relaxation delays were 4 s for (a) and 2.5 s for (b) and (c). A 100 Hz line broadening was applied.
(a) [^{113}Cd]HDH plus 0.5 equiv of L-histidinol per subunit (30,000).
(b) [^{113}Cd]HDH plus 2 equiv of L-histidinol per subunit (120,000).
(c) [^{113}Cd]HDH plus 2 equiv of DL-histidinal per subunit (80,000).

chemical exchange. The line widths were the same for both complexes when measured at 88.8 MHz, although they are different at 133.1 MHz (Table 2-1).

Table 2-1: ^{113}Cd chemical shift of [^{113}Cd]HDH in the presence of ligands

ligand	δ(ppm)	line width (Hz)[a]
no	110	400 (280)[b]
NAD^+	108	400
substrate		
L-histidinol	210	580 (350)[b]
DL-histidinal	192	480 (350)[b]
inhibitor		
imidazole	142	550
+NAD^+	100	400
histamine[c]	152	430
L-histidine[c]	190	480
DL-4-(4-imidazolyl) -3-amino-2-butanone[c]	220	450

a) Values are obtained at 133.1 MHz

b) Values in parentheses are values of line width at 88.8 MHz

c) There was no significant difference in the presence of NAD^+.

In the absence of substrates, the addition of NAD^+ to [^{113}Cd]HDH made the resonance of [^{113}Cd]HDH shift slightly to upfield (108 ppm) without changing the line width (spectrum not shown).

^{113}Cd NMR spectrum of [^{113}Cd]HDH-histidinol complex in the presence of $^{113}Cd^{2+}$. A substrate for HDH, L-histidinol, was added to the solution of [^{113}Cd]HDH containing excess $^{113}Cd^{2+}$ ions. The ^{113}Cd resonance of the complex in the presence of $^{113}Cd^{2+}$ showed a resonance at 210 ppm, which was identical to the result in Figure 2-5b, and the line width of the complex was also similar to that in the absence of the excess metal ions (data not shown). The large downfield shift of the original site indicates that the substrate interacts with the metal ion in the original site, and there is little difference of [^{113}Cd]HDH-histidinol complex in between the presence and absence of $^{113}Cd^{2+}$. On the other hand, the peaks of A', A", and B sites $^{113}Cd^{2+}$ disappeared, indicating that these sites are also influenced by the addition of the substrate. It is not apparent whether $^{113}Cd^{2+}$ ions of A' and A" sites contribute to the peak at 210 ppm, or the peaks of these two sites were broadened by chemical exchange such as local conformational fluctuation, ligand exchange.

^{113}Cd NMR of binary [^{113}Cd]HDH-inhibitor and ternary [^{113}Cd]HDH-NAD^+-inhibitor complexes. The binary and ternary complexes of [^{113}Cd]HDH-inhibitor were examined for following compounds; imidazole, histamine, L-histidine, and DL-4-(4-imidazolyl)-3-amino-2-butanone (Scheme 2-2). These compounds were known as competitive inhibitors for [Zn]HDH, and *K*i values for imidazole and L-histidine are about 1 mM, and those for histamine and DL-4-(4-imidazolyl)-3-amino-2-butanone are 35 and 5 μM, respectively (Grubmeyer et al., 1989). Figure 2-6 shows ^{113}Cd NMR spectra of [^{113}Cd]HDH in the complex with the inhibitor in the absence and presence of NAD^+. *K*m value for NAD^+ is 50 μM (Nagai et al., 1992).

Scheme 2-2: HDH inhibitors.

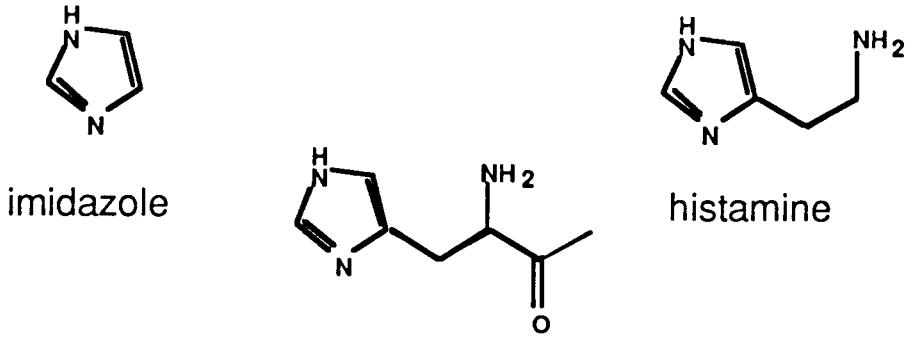

All the ^{113}Cd NMR results for the [^{113}Cd]HDH-inhibitor complexes are summarized in Table 2-1. It was confirmed that these shifts were unchanged when the NMR measurements were carried out for up to 5-fold concentration of the ligand to the enzyme.

^{113}Cd NMR resonance of the binary [113Cd]HDH-imidazole complex was observed at 142 ppm (Figure 2-6a). The addition of NAD^+ to the binary complex made the peak shift back to 100 ppm (Figure 2-6b).

As for the other three inhibitors (histamine, L-histidine, and DL-4-(4-imidazolyl)-3-amino-2-butanone), the binary complex showed a resonance at 153, 190 and 220 ppm (Figure 2-6c, d, and e), respectively. The ternary complex of the inhibitors, however, gave an identical resonance to the corresponding binary complex (spectra not shown). Consequently, the addition of NAD^+ did not change the spectra of the binary complex of the inhibitors except that of imidazole.

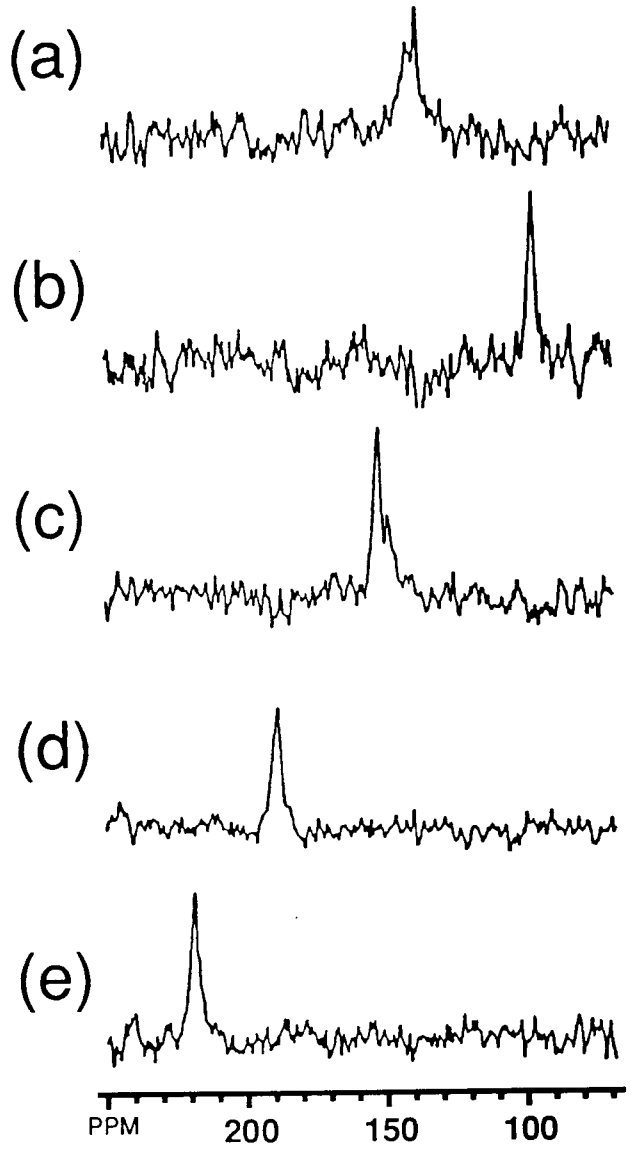

Figure 2-6: ^{113}Cd NMR spectra of the [^{113}Cd]HDH-inhibitor complexes in 20 mM Tris-SO_4, 20 °C. The number of scans is given in the parentheses. The relaxation delays were 2.5 s for all spectra. A 100 Hz line broadening was applied.
(a) [^{113}Cd]HDH plus 10 equiv of imidazole per subunit (30,000).
(b) (a) plus 2 equiv of NAD+ per subunit.
(c) [^{113}Cd]HDH plus 2 equiv of histamine per subunit (50,000).
(d) [^{113}Cd]HDH plus 10 equiv of L-histidine per subunit (60,000).
(e) [^{113}Cd]HDH plus 4 equiv of DL-4-(4-imidazolyl)-3-amino-2-butanone per subunit (50,000). The signal at 140 ppm is an artifact in (a) and (b).

Discussion

Interaction of the metal ion with substrate and inhibitor. The significant shifts of [^{113}Cd]HDH resonance in the presence of the ligand suggest that the substrates or inhibitors, except NAD^+, interact with the metal ion, and that the metal binding site of HDH is located in the catalytic site. For small metalloenzymes, ^{1}H-^{113}Cd heteronuclear multiple quantum coherence (HMQC) experiment provides unambiguous evidence for ligand binding to the metal ion (see Summers, 1988). However, HMQC spectra of [^{113}Cd]HDH with various delay periods did not show any peaks (data not shown). Thus, although it is indirect, the ^{113}Cd chemical shifts of [^{113}Cd]HDH in the presence and absence of the substrates and inhibitors would provide us with information about coordinated ligands.

Downfield shifts of the binary [^{113}Cd]HDH-imidazole and -histamine complexes from [^{113}Cd]HDH were 32 and 42 ppm, respectively. The calculated downfield shift of the coordination of imidazole to ^{113}Cd is 42 ppm, and that of primary amino group is 73 ppm (Summers, 1988). The coordination of imidazole exhibited 36 ppm downfield shift in ^{113}Cd NMR study of LADH (Bobsein & Myers, 1980). These results indicate that the imidazole portion of the HDH ligands is coordinated to the metal ion, but the amino group is not. HDH shows a high degree of substrate specificity that arises from specific binding interactions. It was reported that the imidazole portion of the binding site contributes considerably to the overall binding energy and is highly specific, and that most of the side-chain binding interaction occurs at the amino group (Grubmeyer et al., 1989). Figure 2-7 is a schematic drawing of the metal binding site of HDH in the complex with the ligand derived from the ^{113}Cd NMR data. Since the amino group of the ligands is known as a critical binding

portion for HDH (Grubmeyer et al., 1989), it may interact with the other part of the protein.

The other complexes (L-histidinol, DL-histidinal, L-histidine and DL-4-(4-imidazolyl)-3-amino-2-butanone) showed diverse downfield shifts (38-65 ppm) from the [^{113}Cd]HDH-histamine complex. It indicates that the environment around the metal ion is sensitive to difference in the chemical structure of functional groups (X in Figure 2-7), and suggests that besides the imidazole portion of the ligands, an oxygen atom of the functional group X also interacts with the metal ion. It is possible that the metal ion plays a similar role as a Lewis acid like the Zn(II) in LADH, inducing polarization of the carbonyl group to increase the susceptibility to nucleophile attack for the aldehyde oxidation. The differences in electronegativities and location of the oxygen atoms may cause the diverse downfield shifts. Taking into account the coordination of the imidazole portion, the coordination number might be five in the transition state of HDH reaction.

The metal ion would be involved in the catalytic reaction of HDH. ^{113}Cd NMR results of ^{113}Cd-substituted HDH reveal that the metal ion is located in the catalytic site. The involvement of the metal ion in the catalytic reactions was demonstrated by the chemical shift changes of [^{113}Cd]HDH-ligand complexes, although the conformational change induced by ligand binding may contribute to the chemical shift changes of the complexes to some extent.

NAD+ binding site. ^{113}Cd chemical shift of the ternary complex of [^{113}Cd]HDH-inhibitor-NAD$^+$ is identical to that of the corresponding binary complex except for that of imidazole. This means that the enzyme structure around the metal binding site of the binary [^{113}Cd]HDH-inhibitor complex remains unchanged by the binding of NAD$^+$. ^{113}Cd NMR studies on LADH showed that the NAD$^+$ binding to the catalytic

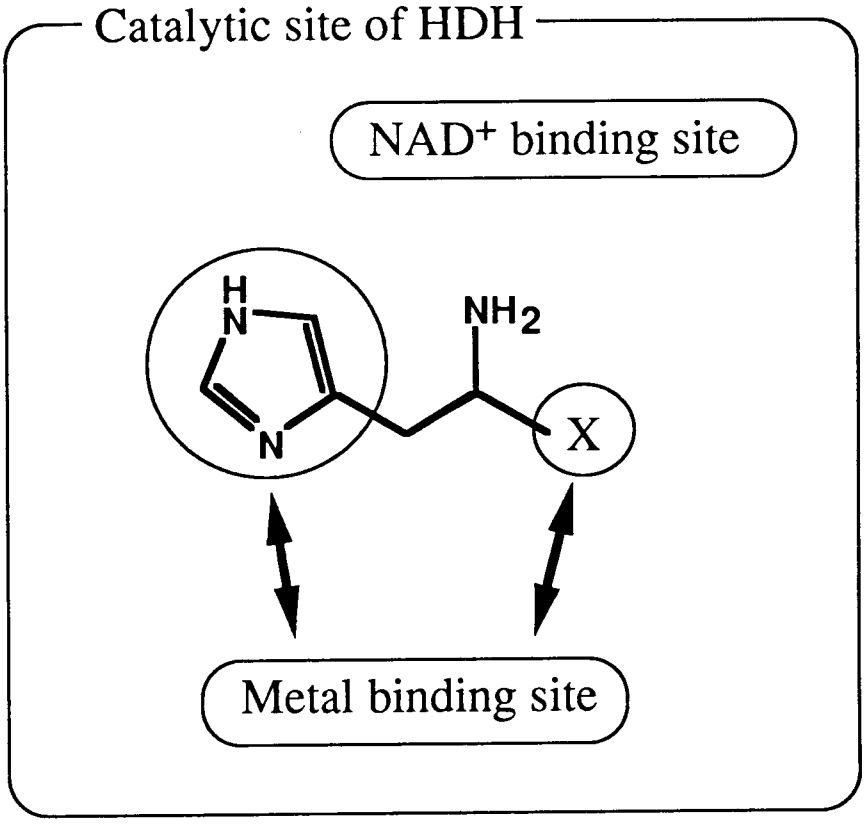

Figure 2-7: A schematic drawing of HDH catalytic site with a ligand. Arrows indicate the interaction between the metal binding site and the functional group of the ligand. X = CH_2OH, CHO, COOH, and $COCH_3$.

site of LADH caused an upfield shift of ^{113}Cd resonance due to the conformational change (Bobsein & Myers, 1981). There is no remarkable structural similarity between HDH and LADH, and the reaction order of the alcohol oxidation by HDH differs from that by LADH (Eklund et al., 1986; Zeppezauer, 1986; Coleman, 1992). Relative location of the NAD^+ and metal binding sites would be different between HDH and LADH. The exceptional upfield shift of the [^{113}Cd]HDH-imidazole-NAD^+ complex from its binary complex indicates the dissociation of the coordination bond. The lack of the amino group may destabilize the binary complex.

Residues coordinated to the catalytic metal ion. It is empirically known that metal binding sites comprising exclusively O-donor ligands give ^{113}Cd signals in the range +40 to -180 ppm, sites with one to three N donors give shifts in the range 40 to ca. 300 ppm, and sites with S donors give signals with shifts from ca. 400 to 800 ppm (Summers, 1988). The chemical shift (110 ppm) of [^{113}Cd]HDH in the absence of the substrates and inhibitors excludes the possibility of sulfur ligation and an all-oxygen ligand set of the protein residues. This result is consistent with the site-specific mutagenesis studies that the conserved cysteine residues are not liganded to the metal ion (Teng et al., 1993; Nagai et al., 1993). Thus, the metal ion in [^{113}Cd]HDH is coordinated to the protein by a combination of nitrogen and oxygen ligands. Examples of such a metal site are listed in Table 2-2 by a tabulation of the ^{113}Cd chemical shifts available for ^{113}Cd-substituted protein whose ligand set was determined by X-ray crystallography, suggesting that the metal binding site of [^{113}Cd]HDH contains two nitrogens, most probably His, and oxygen ligands such as Asp, Glu.

Table 2-2: ^{113}Cd chemical shift of ^{113}Cd-substituted proteins whose ligand set is composed of nitrogen and oxygen[a)]

protein	δ(ppm)	ligand set[b)]
Alkaline phosphatase	52	N 2COO W
Concanavalin A	32-46	N 3COO 2W
Carboxypeptidase A	120	2N COO W
Insulin	165	3N 3W
Carbonic anhydrase	210-220	3N W

a) from Summers, (1988)

b) N = imidazole, COO = carboxyl, and W = water molecule

These results are in accord with a general ligand rule for the catalytic zinc ion, in which His is by far the most common ligand, while Cys is not (Table 2-3; Vallee & Auld, 1990a,b). Horse liver alcohol dehydrogenase (LADH) is known as an exception of the general ligand rule. One of two metal ions in LADH is located in the catalytic site, where one H_2O, one His, and two Cys are coordinated to the metal ion (Eklund et al., 1976).

With a few exceptions (e.g. LADH), a systematic spacing in sequence of the metal ligands is observed for the active zinc site of the zinc enzymes (Table 2-3): The first two ligands are separated by a "short spacer" consisting of 1 to 3 amino acids, and these ligands are separated from the third ligand by a "long spacer" of ~20 to ~120 amino acids. HDH follows the general ligand rule of the catalytic zinc site like usual zinc enzymes. Assuming that the metal ligand set of HDH (His and Asp/Glu) follows the systematic spacing, a pair of His^{261}-Asp^{264} only satisfies the condition of the short spacer in all the pairs of conserved His-Asp, His-Glu, and His-His (Nagai et al., 1991). Recently, it was reported that His^{261} is essential

for the ligation of the zinc of *Cabbage* HDH (Nagai & Ohta, 1994). Therefore, Asp^{264} would also be a metal ligand of HDH. The rest of conserved His residues, His^{327} and His^{367} satisfy the condition of the long spacer. Since it was confirmed that His^{367} is not essential for biological activity of HDH (Nagai & Ohta, 1994), His^{327} might be one of the protein residues of the metal ligands .

Table 2-3: Zinc ligands and their spacing for the catalytic zinc[a)]

Enzyme	L_1	X	L_2	Y	L_3	L_4[b)]
Carbonic anhydrase I	His	1	His	22	His(C)	H_2O
Carbonic anhydrase II	His	1	His	22	His(C)	H_2O
β-Lactamase	His	1	His	121	His(C)	H_2O
DD-Carboxypeptidase	His	2	His	40	His(N)	H_2O
Thermolysin	His	3	His	19	Glu(C)	H_2O
B.cereus neutral protease	His	3	His	19	Glu(C)	H_2O
Carboxypeptidase A	His	2	Glu	123	His(C)	H_2O
Carboxypeptidase B	His	2	Glu	123	His(C)	H_2O
Phospholipase C	His	3	Glu	13	His(N)	H_2O
Alkaline phosphatase	Asp	3	His	80	His(C)	H_2O
Alcohol dehydrogenase	Cys	20	His	106	Cys(C)	H_2O

a) from Vallee and Auld (1990a)

b) X is the number of amino acids between L_1 and L_2: Y is the number of amino acids between L_3 and its nearest zinc ligand neighbor. L_3 comes from either the amino (N) or the carboxyl (C) portion of the protein.

One water molecule is generally coordinated to the catalytically active Zn(II) ions of zinc metalloenzymes, and exhibits a critical component (Vallee & Auld, 1990a,b). Provided that the metal ion is located in the catalytic site, it is expected that H_2O is coordinated to the metal ion of HDH. The fact that H_2O is involved in the catalytic reaction (Scheme 2-1) also supports the coordination of H_2O. The coordinated water molecule would not readily be exchangeable with solvent water molecules by taking into account that the chemical shift of [^{113}Cd]HDH is not affected by chloride ion concentration.

Enhancement of catalytic activity by pH and excess Cd^{2+} ions. The resonance of [^{113}Cd]HDH broadened with an increase of pH (Figure 2-2). Such a broadening feature can be explained by a small population of other Cd(II) species (Gettins, 1986). The signal broadening of [^{113}Cd]HDH with an increase of pH would be attributed to an intermediate exchange process between at least two environments around the metal ion. The enzymatic activity of HDH is enhanced with increasing pH, and becomes the highest at pH 9.2 where all the catalytic parameters (e.g. *K*m, *k*cat) were determined (Nagai & Scheidegger, 1991). The facts that the metal ion of HDH is removed by EDTA at pH 9.2 but not at neutral pH (Nagai & Ohta, 1994) suggest conformational fluctuations around the catalytic site at the higher pH, which allow the substrate or EDTA molecules to easily access to the metal ion.

The stimulatory effect by metal ions in the medium has been known to be specific for Mn^{2+}, but the mechanism has not been manifested yet (Grubmeyer et al., 1989; Teng et al., 1993). We found that, like Mn^{2+}, Cd^{2+} ions in the medium interact with the protein, and stimulate HDH reaction. Specific binding of metal ions to the protein besides the catalytic binding site would induce conformational change, resulting in the conformational heterogeneity around the catalytic metal binding site: there are at least three discernible states of the enzyme in which the

environment of the catalytic site differs as represented by A, A', and A" site under this condition. The removal of the excess $^{113}Cd^{2+}$ ions by EDTA would result in simultaneous disappearance of A' and A" sites, and make all the protein molecules reversibly take the major HDH conformation in the absence of the excess metal ion, represented by the peak at 110 ppm (Figure 2-4a). The affinity of Cd^{2+} for this particular binding site is probably lower than that of Cd^{2+} for the catalytic metal binding sites (A, A', and A"). The exchange process resulting in line broadening or the binding of Cd^{2+} to the rigid part of the enzyme resulting in longer longitudinal relaxation time would make detection of ^{113}Cd signal at this binding site difficult.

As judged by the chemical shift, Cd^{2+} ion in A' and A" site (83 and 22 ppm) should be coordinated to nitrogen and oxygen ligands, and B site may consist of all-oxygen ligand set (Summers, 1988). As compared to A site (110 ppm), it is possible that the above-mentioned structural change includes the substitution of the residues coordinated to the metal ion, in particular, for A" site Cd^{2+}. It is reported that one of the conserved cysteine residues (Cys^{116} for *Salmonella typhimurium*, Cys^{112} for *Cabbage* HDH) may be adjacent to the metal in metal binding site but not liganded to it (Teng et al., 1993). ^{113}Cd chemical shifts of these additional sites (83 and 22 ppm) exclude the possibility for sulfur ligation that should cause a large downfield shift (> 400 ppm) (Summers, 1988), and demonstrate that the cysteine residue does not ligand to the metal ion after the structural change.

With an increase of the Cd^{2+} concentrations in solution, the catalytic activity of [Zn]HDH was stimulated first, and then gradually inhibited (Figure 2-3). This suggests that the enzyme could take higher and lower active form depending on Cd^{2+} concentration. The three states observed by ^{113}Cd NMR are likely to correspond to these forms although the assignment of the states to more or less active forms is difficult.

Cd^{2+} ions in the catalytic metal binding site, in particular, A site (110 ppm) of [^{113}Cd]HDH were easily exchanged with the metal ions in the

medium (Figure 2-4c and d). This suggests that in the presence of the excess metal ions, conformational fluctuations are increased around the catalytic metal binding site, compared to that in the absence of them. The fluctuations may cause the change in the affinity of the substrate for the catalytic site, leading to the enhancement of the catalytic activity, although the metal ion bound to the protein is essential for the catalytic activity of HDH (Lee & Grubmeyer, 1987). A similar correlation between the catalytic activity and the conformational fluctuation is observed for [Zn]HDH. At pH 9.2, an optimum pH for the catalytic activity of HDH (Nagai & Scheidegger, 1991), Zn^{2+} in [Zn]HDH is replaced by Mn^{2+} in the medium (Teng et al., 1993). The exchange broadening of the ^{113}Cd signal was also observed in the pH titration experiment above pH 8.0 (Figure 2-2). These results suggest that the structural fluctuation around the catalytic metal binding site is closely related to the stimulation of the HDH activity.

2.5 Conclusion

Significant shifts of [^{113}Cd]HDH resonance in the presence of the ligand indicate that the metal ion is located in the catalytic site of HDH, and that substrates and inhibitors interact with the metal ion. The imidazole portion of the HDH ligands is coordinated to the metal ion, but the amino group is not. The amino group may interact with the other part of the protein. Besides the imidazole portion, an oxygen atom of the functional group such as, hydroxyl group of histidinol, aldehyde group of histidinal also interacts with the metal ion. On the other hand, the NAD^+ binding site may be apart from the metal binding site, and the metal-ligand complex is not influenced by the NAD^+ binding. The ^{113}Cd NMR study of [^{113}Cd]HDH also showed that the metal ion is bound to the protein by a combination of nitrogen and oxygen ligands.

It is also demonstrated that the enhancement of the enzymatic reaction of HDH by the addition of Cd^{2+} ion to the reaction mixture was closely related to the catalytic metal binding site. $^{113}Cd^{2+}$ ion less than 1 equiv per subunit binds to the original Zn^{2+} site of the apoenzyme, while the interaction of excess metal ions with HDH causes structural change and fluctuation around the catalytic metal site. It was confirmed that at least two conformations different from the native conformation are induced by the addition of the excess metal ions. The structure fluctuation would be related to the change of the catalytic activity.

This is the first report about the role of the metal ion of HDH. The information about interaction between the metal ion and ligand will be useful for design of strong inhibitors, which may be a lead compound of herbicide.

2.6 References

Adams, E. (1955) *J. Biol. Chem. 217*, 25-344.

Bobsein, B. R., & Myers, R. J. (1980) *J. Am. Chem. Soc. 102*, 2454-2455.

Bobsein, B. R., & Myers, R. J. (1981) *J. Biol. Chem. 256*, 5313-5316.

Bürger, E., & Görisch, H. (1981) *Eur. J. Biochem 118*, 125-130.

Chlebowski, J. F., & Coleman, J. E. (1976) *J. Biol. Chem. 251*, 1202-1206.

Coleman, J. E. (1992) *Annu. Rev. Biochem. 61*, 897-946.

Dess, D. B., & Martin, J. C., (1983) *J. Org. Chem. 48*, 4155-4156.

Eklund, H., Nordström, B., Zeppezauer, E., Söderlund, G., Ohlson, I., Boiwe, T., Söderberg, B.-O., Tapia, O., Brändén, C.-I., & Åkeson, Å. (1976) *J. Mol. Biol. 102*, 27-59.

Eklund, H., Jones, A., & Schneider, G. (1986) *in Zinc Enzymes* (Bertini, I., Luchinat, C., Maret, W., Zeppezauer, M., Ed.) pp 377-392, Birkhauser, Boston, MA.

Gettins, P. (1986) *J. Biol. Chem. 261*, 15513-15518.

Grubmeyer, C. T., Chu, K. W., & Insinga, S. (1987) *Biochemistry 26*, 3369-3373.

Grubmeyer, C. T., Insinga, S., Bhatia, M., & Moazami, N. (1989) *Biochemistry 28*, 8174-8180.

Grubmeyer, C., Skiadopoulos, M. and Senior, A. E. (1989) *Arch. Biochem. Biophys. 272*, 311-317.

Kheirolomoom, A., Mano, J., Nagai, A., Ogawa, A., Iwasaki, G., & Ohta, D. (1994) *Arch. Biochem. Biophys. 312*, 493-500.

Laemmli, U. K. (1970) *Nature 227*, 680-685.

Lee, S. Y., & Grubmeyer, C. T. (1987) *J. Bacteriol. 169*, 3938-3944.

Loper, J. C. and Adams, E. (1965) *J. Biol. Chem. 240*, 788-795.

Mancuso, .A. J., Uuang, S. -L., & Swern, D. (1978) *J. Org. Chem. 43*, 2480-2482.

Nagai, A., & Scheidegger, A., (1991) *Arch. Biochem. Biophys. 284*, 127-132.

Nagai, A., Ward, E., Beck, J., Tada, S., Chang, J.-Y., Scheidegger, A., & Ryals, J. (1991) *Proc. Natl. Acad. Sci. U. S. A. 88*, 4133-4137.

Nagai, A., Suzuki, K., Ward, E., Moyer, M., Hashimoto, M., Mano, J., Ohta, D., & Scheidegger, A. (1992) *Arch. Biochem. Biophys. 295*, 235-239.

Nagai, A., Kheirolomoom, A., & Ohta, D. (1993) *J. Biochem. 114*, 856-861.

Nagai, A., & Ohta, D. (1994) *J. Biochem. 115*, 22-25.

Omburo, G. A., Mullins, L. S., & Raushel,. F. M. (1993) *Biochemistry 32,* 9148-9155.

Otvos, J. D. and Armitage, I. M. (1980) *Biochemistry 19,* 4031-4043.

Pan, T., Freedman, L. P. and Coleman, J. E. (1990) *Biochemistry 29,* 9218-9225.

Smissman, E. E., & Weis, J. A. (1971) *J. Med. Chem. 14,* 945-947.

Sudmeier, J. L., Bell, S. J., Storm, M. C. and Dunn, M. F. (1981) *Science 212,* 560-562.

Summers, M. D., & Smith, G. E. (1987) in *A Manual of Methods for Baculovirus Vectors & Insect Cell Culture Procedures, Bulletin No. 1555*, Texas Agricultural Experiment Station & Texas A&M University, College Station, TX.

Summers, M. F. (1988) *Coord. Chem. Rev. 86*, 43-134.

Teng, H., Segura, E., & Grubmeyer, C. (1993) *J. Biol. Chem. 268*, 14182-14188.

Vallee, B. L., & Auld, D. S. (1990a) *Proc. Natl. Acad. Sci. U. S. A. 87*, 220-224.

Vallee, B. L., & Auld, D. S. (1990b) *Biochemistry 29*, 5647-5659.

Zeppezauer, M. (1986) *in Zinc Enzymes* (Bertini, I., Luchinat, C., Maret, W., Zeppezauer, M., Ed.) pp 417-434, Birkhauser, Boston, MA.

Summary

In this thesis, significant and unique information is obtained by NMR spectroscopy for the biological systems where the precise structure determination can not be performed. From an applied biological point of view, the clarified fibrillation mechanism in Chapter 1 provides us with a clue of the synthesis of modified peptides which is stable in solution, and the elucidation of the interaction of the substrate with the catalytic metal ion in Chapter 2 is significant for the inhibitor design by a combined use of database search.

Since it takes 10~15 billion yen and 10~15 years to develop a new drug to market, effective investigation on a target molecule will be more and more indispensable for pharmaceutical companies, and from now on, NMR will be frequently applied to research and development of pharmaceutical and agricultural medicine. Taking into consideration of competition with X-ray crystallography in the field of the precise tertiary structural determination, NMR will be more important for studies, such as, dynamics of biological molecules, protein folding-unfolding, interaction of weak affinity ligands with enzymes, and so on. The investigation on the peptide aggregation in this thesis which cannot be performed by X-ray crystallography, is one of the original targets for NMR spectroscopy.

List of Publications

Chapter 1

Kanaori, K., & Nosaka, Y. A. (1995) *Biochemistry 34,* 12138-12143.

Kanaori, K., & Nosaka, Y. A. (1995) *Bull. Magn. Reson. 17,* 274-275.

Kanaori, K., & Nosaka, Y. A. (1996) *Biochemistry* in press.

Chapter 2

Kanaori, K., Uodome, N., Nagai, A., Ohta, D., Ogawa, A., Iwasaki, G., & Nosaka, Y. A. (1996) *Biochemistry 35,* 5949-5954.

Kanaori, K., & Nosaka, Y. A. (1996) *manuscript in preparation (to FEBS Lett.)*

Publications not included in this thesis

Tamura, A., Kanaori, K., Kojima, S., Kumagai, I., Miura, K., & Akasaka, K. (1991) *Biochemistry 30,* 5275-5286.

Monma, K., Hatanaka, T., Inouye, K., Kanaori, K., Tamura, A., Akasaka, K., Kojima, S., Kumagai, I., Miura, K., & Tonomura, B. (1993) *J. Biochem. 114,* 553-559.

Konno, T., Kataoka, M., Kamatari, Y., Kanaori, K., Nosaka, A., & Akasaka, K. (1995) *J. Mol. Biol. 251,* 95-103.

Acknowledgments

The present investigation was carried out under the guidance of Dr. Atsuko Yamada Nosaka at the Analytics & Informatics Department (now Core Technology Unit), International Research Laboratories, Ciba-Geigy Japan Ltd. from 1991 to 1995. The author wishes to express his thanks to her for her constant guidance and valuable discussions throughout this work.

The author is deeply indebted to Professor Kazuyuki Akasaka at the Department of Chemistry, Faculty of Science, Kobe University for his encouragement since 1988 when the author was a student of Kyoto University, and for affording the author a chance to obtain the Ph.D. degree.

The author also wishes to extend his hearty thanks to members of IRL, Ciba-Geigy for their kind help and collaboration.

Finally, the author greatly appreciates to my parents and my wife, Kyoko, for encouragement and daily assistant.

May, 1996

Kenji Kanaori